

The Geological Society of America
Special Paper 509
2015

Aftershocks illuminate the 2011 Mineral, Virginia, earthquake causative fault zone and nearby active faults

J. Wright Horton Jr.*

U.S. Geological Survey, MS 926A, 12201 Sunrise Valley Drive, Reston, Virginia 20192, USA

Anjana K. Shah

U.S. Geological Survey, P.O. Box 25046, Denver Federal Center, MS 964, Denver, Colorado 80225, USA

Daniel E. McNamara

U.S. Geological Survey, Geologic Hazards Science Center, 1711 Illinois St., Golden, Colorado 80401, USA

Stephen L. Snyder

U.S. Geological Survey, MS 954, 12201 Sunrise Valley Drive, Reston, Virginia 20192, USA

Aina M. Carter

3391 W. Old Mountain Road, Louisa, Virginia 23093, USA

ABSTRACT

Deployment of temporary seismic stations after the 2011 Mineral, Virginia (USA), earthquake produced a well-recorded aftershock sequence. The majority of aftershocks are in a tabular cluster that delineates the previously unknown Quail fault zone. Quail fault zone aftershocks range from ~3 to 8 km in depth and are in a 1-km-thick zone striking ~036° and dipping ~50°SE, consistent with a 028°, 50°SE main-shock nodal plane having mostly reverse slip. This cluster extends ~10 km along strike. The Quail fault zone projects to the surface in gneiss of the Ordovician Chopawamsic Formation just southeast of the Ordovician–Silurian Ellisville Granodiorite pluton tail. The following three clusters of shallow (<3 km) aftershocks illuminate other faults. (1) An elongate cluster of early aftershocks, ~10 km east of the Quail fault zone, extends 8 km from Fredericks Hall, strikes ~035°–039°, and appears to be roughly vertical. The Fredericks Hall fault may be a strand or splay of the older Lakeside fault zone, which to the south spans a width of several kilometers. (2) A cluster of later aftershocks ~3 km northeast of Cuckoo delineates a fault near the eastern contact of the Ordovician Quantico Formation. (3) An elongate cluster of

*whorton@usgs.gov

late aftershocks ~1 km northwest of the Quail fault zone aftershock cluster delineates the northwest fault (described herein), which is temporally distinct, dips more steeply, and has a more northeastward strike. Some aftershock-illuminated faults coincide with preexisting units or structures evident from radiometric anomalies, suggesting tectonic inheritance or reactivation.

INTRODUCTION

Rapid deployment of temporary seismic stations by multiple institutions after the 23 August 2011, M_w (moment magnitude) 5.8 Mineral, Virginia, earthquake produced the best-recorded aftershock sequence in the eastern United States (see McNamara *et al.*, 2014a). For the first time aftershock data illuminated the causative fault of a significant earthquake in the passive-margin geologic setting of the eastern United States, and smaller aftershock clusters illuminated other active faults.

A passive continental margin is formed by rifting followed by seafloor spreading such that the resulting tectonic plate consists of both continental and oceanic lithosphere. The Atlantic margin of North America is among the more widely studied and geologically understood of modern passive margins (Bradley, 2008). Despite this intense study, significant earthquakes in passive-margin settings are less frequent than those on plate margins and not as well studied or recorded by robust seismic networks.

Throughout the eastern United States, historical seismicity, geomorphic data, and paleoseismic data reveal active but poorly understood tectonic processes within areas such as the Central Virginia seismic zone (Pazzaglia and Gardner, 1994; Pazzaglia and Brandon, 1996; Wolin *et al.*, 2012). Intraplate seismicity is commonly assumed to occur along preexisting zones of weakness from ancient plate collisions and rifting that happen to be favorably oriented with respect to the present stress field (Sykes, 1978). Possible causes of stress that could trigger intraplate seismicity in eastern North America (Stein *et al.*, 1989; Wolin *et al.*, 2012) include plate-wide forces such as ridge push and mantle flow beneath the continent (Zoback, 1992; Ghosh and Holt, 2012) as well as more localized processes such as offshore sediment loading (Calais *et al.*, 2010), postglacial rebound and forebulge subsidence (Stewart *et al.*, 2000), or relaxation of the Appalachian Mountains (Ghosh *et al.*, 2009). However, the conditions that concentrate intraplate seismic activity in particular geographic areas such as the Central Virginia seismic zone remain unclear. The Earth science community lacks a comprehensive tectonic model to explain the distribution of eastern United States seismicity in space and time. Given the infrequent nature of significant earthquakes in the eastern United States, characterizing the aftershock sequence of the Mineral earthquake offers a rare opportunity to improve our understanding of earthquake hazard in this geologic setting.

The M_w 5.8 earthquake on 23 August 2011 in central Virginia was a shallow event (7 ± 2 km) that occurred on a southeast-dipping reverse fault, where the maximum compressive stress is represented by a subhorizontal P-axis trending east-southeast at 102° and plunging 3° (Herrmann, 2011; Chapman, 2013; McNamara *et al.*, 2014a).

This orientation and a previously determined average maximum compressive stress for the Central Virginia seismic zone that trends southeast at 133° and plunges 14° (Kim and Chapman, 2005) indicate that the local stress field is anomalous with respect to the northeast-southwest maximum compressive stresses more typical of eastern North America (Zoback, 1992; Mazzotti and Townend, 2010). These continent-scale stresses attributed to plate-wide forces, such as ridge push and mantle flow, thus appear to be overwhelmed by local effects in the Central Virginia seismic zone, perhaps explaining why the area has earthquakes. Within the Central Virginia seismic zone stress field, the most favorable fault strike for reverse activation is northeast (assuming $\sim 45^\circ$ dip), and numerous Paleozoic and Mesozoic structures in the area have this orientation.

The M_w 5.8 August 2011 earthquake in central Virginia was the largest earthquake to occur in the Appalachian region in more than a century and was felt throughout much of the eastern United States and southeastern Canada, possibly by more people than any other earthquake in U.S. history (Horton and Williams, 2012; Hough, 2012). The large felt-area reported by the U.S. Geological Survey (USGS) Did You Feel It (DYFI) system (Wald *et al.*, 2011) is ~ 10 times the area of a similarly sized earthquake in the western United States due to the relatively low attenuation of seismic waves in the eastern United States (McNamara *et al.*, 2014b). Shaking from the earthquake caused Modified Mercalli Intensity (MMI) VIII damage in the epicentral area (Heller and Carter, this volume), caused the safe shutdown of a nuclear power station (Graizer *et al.*, 2013; Li *et al.*, this volume), damaged buildings and monuments 160 km away in Washington, D.C., and caused building evacuations as far as New York City (Earthquake Engineering Research Institute, 2011; Horton and Williams, 2012).

The 2011 Mineral earthquake is the largest magnitude earthquake on record in the Central Virginia seismic zone (Fig. 1), an area of persistent seismic activity in the Piedmont Province between Richmond and Charlottesville (Bollinger and Hopper, 1971; Algermissen and Perkins, 1976; Tarr and Wheeler, 2006; Chapman, 2013). Investigations in the Central Virginia seismic zone prior to this event had been unable to conclusively tie earthquakes to a causative fault. The 23 August 2011 Virginia earthquake provided a rare opportunity for multidisciplinary studies involving modern seismic instruments and methods, geologic mapping, geophysical imaging, and paleoseismic investigations to improve the understanding of earthquakes in the eastern United States and how they may relate to preexisting geologic structures.

The rapid deployment of temporary seismic stations after the 23 August 2011 Virginia earthquake was a cooperative effort that

Aftershocks illuminate the 2011 Mineral, Virginia, earthquake causative fault zone

was led by the USGS and included Virginia Polytechnic Institute and State University, Lamont-Doherty Earth Observatory of Columbia University, University of Memphis Center for Earthquake Research and Information, Lehigh University, and Incorporated Research Institutions for Seismology; 46 3-component seismographs were deployed in the area within five days. Of these 46 seismographs, eight were installed within 24 h, in time

to record the largest aftershock of the sequence (M_w 3.9) on 25 August. Cornell University added more than 200 single-component recorders by 1 September 2011 for a short-term experiment in aftershock imaging with dense arrays (Brown et al., 2012). There were 36 3-component stations in place through early 2012, and a few remained a year after the event. High-quality aftershock data from this instrument array imaged the causative fault of a significant earthquake and illuminated nearby faults. The USGS reported at least 450 aftershocks greater than $M = \sim 1.0$; none of these were greater in magnitude than $M_w = 4.0$, and 7 were $M_w = 3.0$ – 3.9 (McNamara et al., 2014a, Table S2 therein). Earthquakes with magnitudes between 0.5 and 1.0 have not been fully tallied, but probably number in the hundreds to thousands given the magnitude-frequency distribution (b -value = 0.75; determined by McNamara et al., 2014a).

This paper presents the first comprehensive analysis of the M_w 5.8 Mineral, Virginia, earthquake causative fault and subsidiary faults as illuminated by aftershocks with respect to the detailed geologic and tectonic setting. It takes a step toward addressing the longstanding question of whether and how pre-existing geological structures, including older faults, influence intraplate seismicity and earthquake hazards in eastern North America. The high-quality aftershock data offer an unprecedented opportunity to evaluate this earthquake sequence in relation to pre-existing geologic structures and broader implications for intraplate seismic hazards in eastern North America. Aftershocks illuminate the main-shock causative fault and other faults in the vicinity, making it potentially possible to relate geological structures mapped at the surface and inferred from geophysical surveys to a seismogenic fault at depth.

Understanding the connection between local geologic structure and the regional tectonics is important for understanding earthquake hazards. Considerable scientific attention has been paid to plate boundary regions that have undergone relatively frequent large and damaging earthquakes. As demonstrated by the 2011 Mineral, Virginia, earthquake, the 1886 Charleston, South Carolina, earthquake, and other events (Horton et al., this volume, Chapter 1), the passive continental margin of eastern North America can also produce large and damaging earthquakes. This fact is of particular concern to government planners and emergency responders given the large and relatively unprepared population centers.

Results from this and similar studies in the eastern United States are rare and important for the improvement of models describing earthquake risk in a passive-margin tectonic setting. Knowing the distribution of active faults is important to simulate strong ground shaking for hazard mitigation planning and the calculation of probabilistic assessments of seismic hazard, such as the USGS national seismic hazard maps that are used for seismic provisions in building codes (Petersen et al., 2008).

GEOLOGIC SETTING

The M_w 5.8 Mineral earthquake and its aftershocks occurred in a relatively small area (<400 km²) within the much larger

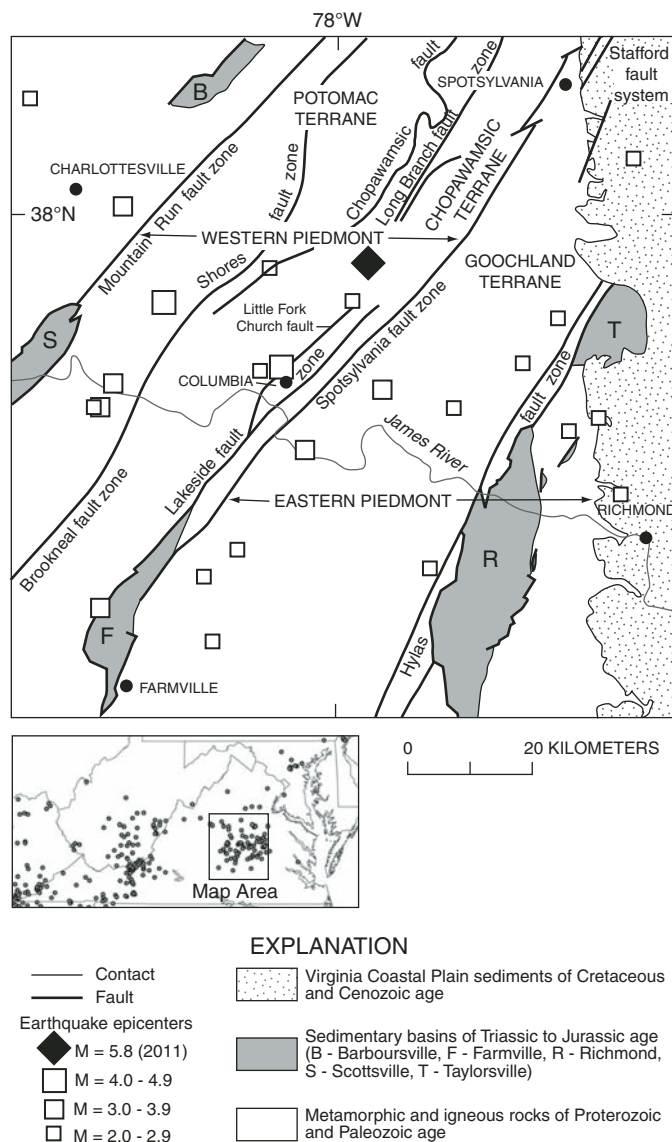


Figure 1. Map of the Central Virginia seismic zone showing tectonic setting and earthquake epicenters (magnitude ≥ 2 from 1973 to 2010, and moment magnitude M_w 5.8 in 2011; aftershocks near the 2011 main shock are not shown). Inset shows map area in relation to epicenters in and near Virginia (magnitude >0 , July 1977–December 2005; from Chapman et al., 2006). The Central Virginia seismic zone is defined by a scattered distribution of earthquakes without a distinct boundary. Earthquakes prior to 2011 show no clear relation to pre-existing faults on the map. Modified from Bailey (2004) and Horton et al. (2014).

(~8000 km²) Central Virginia seismic zone. The earthquake and aftershocks were in gneiss, schist, and intrusive rocks of the Ordovician Chopawamsic terrane (volcanic arc) and nearby rocks (discussed herein), west of the late Paleozoic dextral transpressional strike-slip Spotsylvania fault zone (Bailey et al., 2004) and southeast of the early Paleozoic Chopawamsic thrust fault (Hughes et al., 2013) shown in Figure 1. The rocks contain multiple foliations and fold generations attributed to Paleozoic orogenic events (Burton et al., 2014, this volume). Other faults that project into the area (Fig. 1) include the Long Branch thrust fault (east dipping with dextral component), the Little Fork Church fault (thrust), and the Lakeside fault zone, which is a late Paleozoic dextral mylonite zone reactivated during the early Mesozoic as a normal fault (Wilkes, 1982; Mixon et al., 2000; Spears et al., 2004; Spears, 2011; Horton et al., 2014a). Jurassic diabase dikes of the Central Atlantic Magmatic Province were emplaced during opening of the Atlantic Ocean and, in this area, are typically subvertical and strike north-northeast to north-northwest (McHone, 1988, 2000; Virginia Division of Mineral Resources, 1993). Most earthquakes recorded throughout the Central Virginia seismic zone have upper crustal focal depths of <11 km (Bollinger and Sibol, 1985), and the nearby Interstate Highway I-64 seismic reflection profile shows gently southeast dipping reflector packages interpreted to represent thrust sheets of metamorphic and igneous rocks at similar depths (Pratt et al., 1988, this volume). Outcrop-scale brittle faults and fractures are common in the area (e.g., Bailey and Owens, 2012) but have not been studied in detail.

It may be noteworthy that early Mesozoic extensional basins and cataclastic fault fabrics are commonly but not invariably localized along earlier Paleozoic ductile shear zones containing mylonitic rocks in eastern North America (Swanson, 1986). This tectonic inheritance is exemplified in Virginia by the Hylas fault zone bordering the Richmond and Taylorsville basins in the eastern Piedmont (Bobyarchick and Glover, 1979), by the Lakeside fault zone bordering the Farmville basin in the central Piedmont (Bourland et al., 1979; Wilkes, 1982; Spears and Bailey, 2002), and by the Chatham fault (and Brookneal fault zone) bordering the Danville basin in the western Piedmont (Robinson, 1979; Gates, 1997).

The late Paleozoic dextral transpressional Spotsylvania fault zone (Fig. 1) separates the Chopawamsic terrane from the Goochland terrane on the east, and extends southwestward beneath the early Mesozoic Farmville rift basin. It was first described as a geophysical lineament (Neuschel, 1970) and later interpreted as a 2–3-km-wide zone of en echelon brittle faults (Pavlides et al., 1980) and as a Paleozoic thrust (Farrar, 1984; Pratt et al., 1988). The zone has multiple strands and variable mylonitic foliation over a width >10 km (Spears et al., 2004). The foliation strikes northeast and generally dips southeast. Structural analysis indicates dextral strike slip with a contractional component and suggests 80–300 km of displacement during the Alleghanian orogeny (Bailey et al., 2004). Brittle faults overprint mylonitic fabrics in the Spotsylvania zone and are commonly attributed to Mesozoic reactivation (Bourland et al., 1979; Spears and Bailey, 2002). Reverse faults of Cretaceous

and Cenozoic age in the Stafford fault system (Fig. 1) overlie a subsurface extension of the Spotsylvania zone beneath the Atlantic coastal plain sediments to the northeast (Powars et al., 2012). An M_w 4.3 earthquake on 9 December 2003 occurred near the Spotsylvania fault zone (Bailey, 2004; Kim and Chapman, 2005), but uncertainty about locations of earthquakes in Virginia has limited evaluation of such associations.

The Lakeside fault zone (Fig. 1) bounds the western edge of the early Mesozoic Farmville rift basin and is generally interpreted as a down-to-the-southeast brittle normal fault. The brittle faults overprint mylonitic fabrics, and the zone of mylonitic foliation strikes northeast, dips gently to moderately southeast, and ranges in width to 5 km (Bourland et al., 1979). The Lakeside fault zone has been mapped northeastward to the vicinity of Interstate Highway I-64 (Virginia Division of Mineral Resources, 1993; Spears et al., 2004, 2013).

The Long Branch fault zone (Fig. 1) strikes northeast and locally separates schists of the Ordovician Quantico Formation (successor basin) from metavolcanic gneiss of the Ordovician Chopawamsic Formation to the northwest (Mixon et al., 2000). Detailed geologic mapping indicates that this fault zone extends across the epicentral area, where it strikes ~046°–048° and is within the Chopawamsic Formation ~1 km northwest of the Quantico Formation contact (Spears et al., 2013; Burton et al., 2014, this volume). Approximately 60 km northeast of the epicentral area (north of Fig. 1), this zone is approximately parallel to, and within 0.5 km of, the Dumfries fault (Cretaceous or younger) of the Stafford fault system (Mixon et al., 2005).

DATA AND METHODS

This study examined spatial and temporal distributions of well-located aftershock hypocenters from the 2011 Mineral, Virginia, earthquake in relation to geologic maps, vertical cross-section projections, and three-dimensional (3D) rotatable plots in order to identify possible spatial relations among aftershock clusters and preexisting geologic structures, including older faults. Such associations were then evaluated in more detail to determine whether preexisting Paleozoic, Mesozoic, or Cenozoic faults could have been reactivated by the main shock or aftershocks.

Main Shock

The 2011 M_w 5.8 Mineral, Virginia, earthquake was recorded by permanent seismic stations in the Advanced National Seismic System (ANSS) backbone network, Incorporated Research Institutions in Seismology (IRIS) transportable array, and regional earthquake monitoring networks (Horton and Williams, 2012). A strong motion accelerometer at the North Anna nuclear power plant recorded the closest known ground motions of the earthquake, where the maximum horizontal acceleration was 0.27 g (0.27 times the acceleration of gravity; Chapman, 2013; Graizer et al., 2013). The next nearest

Aftershocks illuminate the 2011 Mineral, Virginia, earthquake causative fault zone

recording is available from the USGS ANSS station US.CBN, in Corbin, Virginia, 57 km from the epicenter. Horizontal acceleration at US.CBN reached 0.135 g.

Using a hypocentroidal decomposition (HD) algorithm (Jordan and Sverdrup, 1981) for multiple-event analysis, high-precision relative and absolute locations and depths were obtained (McNamara et al., 2014a). The main-shock epicenter was relocated (at 37.920°N, 77.979°W) ~4.4 km southwest of the initial single-event network epicenter (37.936°N, 77.933°W) provided by the ANSS—Center for Earthquake Research and Information (CERI). This main-shock epicenter is located in

Louisa County, Virginia, ~10 km southwest of the town of Mineral and 10 km south-southeast of the town of Louisa (Fig. 2A). The main shock occurred at a relatively shallow focal depth of 7 ± 2 km using the HD method, or 6 ± 2 km based on regional moment tensor (RMT) waveform modeling (McNamara et al., 2014a). The RMT depth is within the uncertainty of HD results, and the 1 km difference reflects different velocity models (McNamara et al., 2014a). The estimated uncertainty in depth of the main shock is ± 2 km, while map-view epicentral uncertainties are relatively small, ± 0.6 km and ± 0.7 km for the semiminor axis and semimajor axis, respectively.

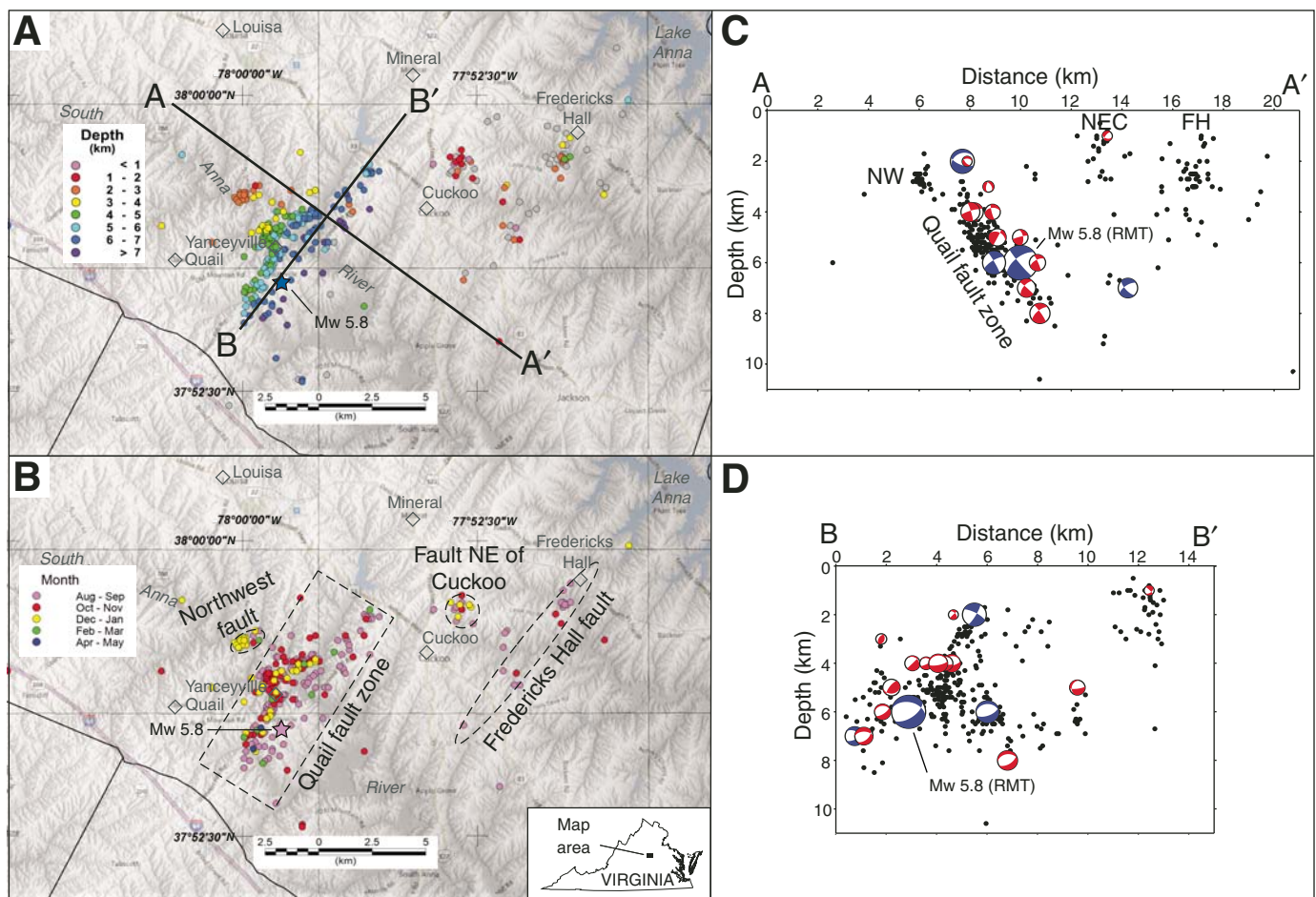


Figure 2. Aftershock-illuminated faults (map and cross sections). (A, B) Maps showing hypocentroidal decomposition (HD) relocated aftershocks (circles) and main shock (star) colored by depth (A) and by month (B) on shaded-relief digital elevation model with roads, water bodies, towns, and labels for aftershock clusters that illuminate active faults. Map A shows all 395 HD-relocated earthquakes regardless of magnitude, distinguishing those having depth uncertainties ≤ 1 km (color) and > 1 km (gray). Map B shows only those earthquakes having depth uncertainties ≤ 1 km. (C, D) Cross sections oriented down-dip (C, A–A') and along strike (D, B–B') of the main, southeast-dipping aftershock cluster show all HD-relocated events and 16 regional moment tensor (RMT) solutions projected onto vertical profiles. Abbreviations: FH—Fredericks Hall fault, NW—northwest fault, NEC—fault northeast of Cuckoo. RMT solutions with compressional quadrants shown in blue represent early events that were located using only data from permanent seismic stations; RMT solutions with compressional quadrants shown in red include data from the temporary aftershock network, and thus are more accurately located. (HD-relocated aftershocks and RMT solutions are from McNamara et al., 2014a.) RMT (beachball) diagrams on the vertical cross sections are oriented with up at the top and down at the bottom, rather than in the standard lower hemisphere projection with north at the top and a vertical center point. Locations: A–A' is from 38.000°N, 78.045°W to 37.890°N, 77.850°W, and B–B' is from 37.900°N, 77.950°W to 37.890°N, 77.850°W.

The main-shock focal mechanism determined from waveform inversion (Herrmann, 2011) shows a nodal plane striking 028° and dipping 50° SE with a rake angle of 113° , consistent with a southeast-dipping planar zone defined by aftershocks (discussed in the following), and mostly reverse (southeast side up) motion (Ellsworth *et al.*, 2011; McNamara *et al.*, 2014a). Ellsworth *et al.* (2011) computed a high-stress-drop main shock (50–75 MPa) on a rupture, 3.2–4.0 km in length, with an average slip of 1.5–2.5 m.

Using detailed waveform modeling, Chapman (2013) showed that the main shock consisted of three subevents having successive focal depths of 8.0 km, 7.3 km, and 7.0 km with estimated uncertainties of ± 1.0 km. The three subevents were initiated near the southwestern end of the main aftershock zone and propagated ~ 2 km northeastward along strike (and ~ 1 km up dip) within 1.6 s (Chapman, 2013).

Aftershocks

This investigation of aftershock distribution from the M_w 5.8 Mineral, Virginia, earthquake in space and time, and in relation to the tectonic setting, is based on a comprehensive catalog of well-located hypocenters (McNamara *et al.*, 2014a). This catalog supersedes preliminary data releases from sources using different seismic instruments and velocity models (Saint Louis University Earthquake Center, 2013; U.S. Geological Survey, 2013). It includes 454 well-recorded earthquakes greater than $M \sim 1.0$ that occurred between 23 August 2011 and 30 July 2012. The highest quality event recordings (395 in number, including the main shock) were relocated using the HD method (McNamara *et al.*, 2014a). This catalog of relocated aftershocks is used herein to analyze aftershock spatial and temporal distributions in relation to geologic structures in the Central Virginia seismic zone.

Figure 2A distinguishes the best located aftershocks, regardless of magnitude, having ≤ 1 km depth uncertainty from those having larger depth uncertainties, whereas Figure 2B shows only the best located aftershocks for comparison and to more sharply delineate particular clusters. The best located aftershocks (having depth uncertainties ≤ 1 km) facilitate more accurate comparisons with geographic locations, geologic features such as preexisting faults, and geophysical expressions of surface and subsurface geology. They are also more reliable for evaluating aftershock depth distributions and 3D geometries of aftershock hypocenter distributions, including dip angles. The remaining aftershocks provide additional documentation of aftershock patterns and clusters with less precision, especially in the vertical direction.

RMT solutions have been determined for 16 of the earthquakes (McNamara *et al.*, 2014a), and with a few exceptions, are consistent with the main-shock rupture on a southeast-dipping reverse fault and parallel southeast-dipping aftershock cluster (Fig. 2C). The most anomalous RMT solution in the main cluster is a shallow M_w 3.9 aftershock on 25 August 2011 that occurred during the passage of Hurricane Irene. Numerous small ruptures represented by after-

shock hypocenters in the main cluster define the Quail fault zone as used here (and in Horton *et al.*, 2012a, 2012b), which extends 10 km along strike (Figs. 2A, 2B) and from ~ 3 to 8 km in depth (Fig. 2C). The HD-relocated main shock is within and near the base of the main aftershock cluster (Figs. 2C, 2D), consistent with the main-shock location of Chapman (2013).

Chapman's (2013) best-fit plane to the main cluster of early aftershocks within nine days of the main shock (no later than 1 September 2011) yielded an inferred fault plane striking 029° and dipping 51° SE, remarkably similar to the USGS–Saint Louis University main-shock moment tensor solution of 028° , 50° SE, rake 113° (Herrmann, 2011). For comparison, a best-fit plane constructed from vertical slices through the entire main cluster of relocated aftershocks (McNamara *et al.*, 2014a) has a mean strike of $036^\circ \pm 12^\circ$ (2σ) and dip of $49.5^\circ \pm 6^\circ$ SE (2σ). Best-fit planes determined for the main aftershock cluster in this study (Appendix) have similar strike and dip of 034.8° , 48.4° SE (including a shallow northwest cluster distinguished in Fig. 2B) or 035.3° , 50.7° SE (excluding the shallow northwest cluster). Closer examination of this main aftershock cluster suggests a tabular zone ~ 1 km thick, rather than a single plane, in which events close together in time are more tightly clustered spatially. Figures 2A and 2B suggest that the northeast part of the main cluster has a more eastward strike than the southwest part, and that dip angles steepen slightly upward (Fig. 2C). Separate best-fit planes, having strike and dip of 029.4° , 61.6° SE for the southwestern part and 047.0° , 58.7° SE for the northeastern part (Appendix), indicate that the Quail fault zone aftershock cluster has a concave-east bend or curve of $\sim 18^\circ$. Separation into these two groups is supported by a root mean squared error of 0.36 for a single plane versus 0.23 and 0.27, respectively, for the separate southwest and northeast planes. If the main aftershock cluster that defines the Quail fault zone steepens upward, then the fault zone would project to the surface slightly southeast of the late shallow northwest cluster of shallow aftershocks.

A rotatable 3D image of main-shock and aftershock hypocenters is available as GSA Data Repository item R1¹, and a time-sequence animation of 369 aftershocks greater than $M \sim 1.0$ recorded through 31 December 2011 is available online (U.S. Geological Survey, 2012).

Geology and Geophysical Imaging

In this study the distributions of well-located aftershocks on maps, cross sections, and 3D rotatable plots were compared to the distribution of known geologic structures such as preexisting faults. Figures 2A and 3 distinguish the best located aftershocks having ≤ 1 km depth uncertainty from those having larger depth

¹GSA Data Repository item 2014379, R1: Rotatable three-dimensional image of the 23 August 2011 Mineral, Virginia, earthquake main-shock and aftershock hypocenters color coded by depth, is available online at <http://www.geosociety.org/pubs/ft2014.htm>, or on request from editing@geosociety.org or Documents Secretary, GSA, P.O. Box 9140, Boulder, CO 80301, USA.

Aftershocks illuminate the 2011 Mineral, Virginia, earthquake causative fault zone

uncertainties; the former provide accurate locations and facilitate comparison with geologic features and geophysical anomalies, and the latter provide additional documentation of aftershock clusters with less precision. Aftershocks shown in Figure 3 (events having magnitude $M \geq 2$) show less scatter than those in Figure 2 (events regardless of magnitude).

Information about the geologic setting (Fig. 3) was compiled from geologic maps (Virginia Division of Mineral Resources, 1993; Pavlides et al., 1994; Mixon et al., 2000; Marr, 2002; Spears et al., 2004; Hughes and Hibbard, 2012a), and supplemented by preliminary findings of geologic mapping (Spears and Gilmer, 2012;

Spears et al., 2013; Hughes et al., 2013, and references therein; Burton et al., 2014), and preliminary interpretations of geophysical data (Zietz et al., 1977; U.S. Geological Survey and National Geophysical Data Center, 2002; Snyder, 2005; Shah et al., 2012a, 2012b, 2012c). Additional sources for surface and subsurface geology include Pratt et al. (1988), Pavlides (1989), Horton et al. (1989, 1991, 2010, 2014a), Thomas (2006), and Hibbard et al. (2007, 2014) for tectonic framework; Spears et al. (2004), Bailey and Owens (2012), Hughes and Hibbard (2012b), and Hughes et al. (2013) for central Virginia Piedmont geology; Gates et al. (1988), and Bailey et al. (2004) for Paleozoic ductile faults; Lindholm

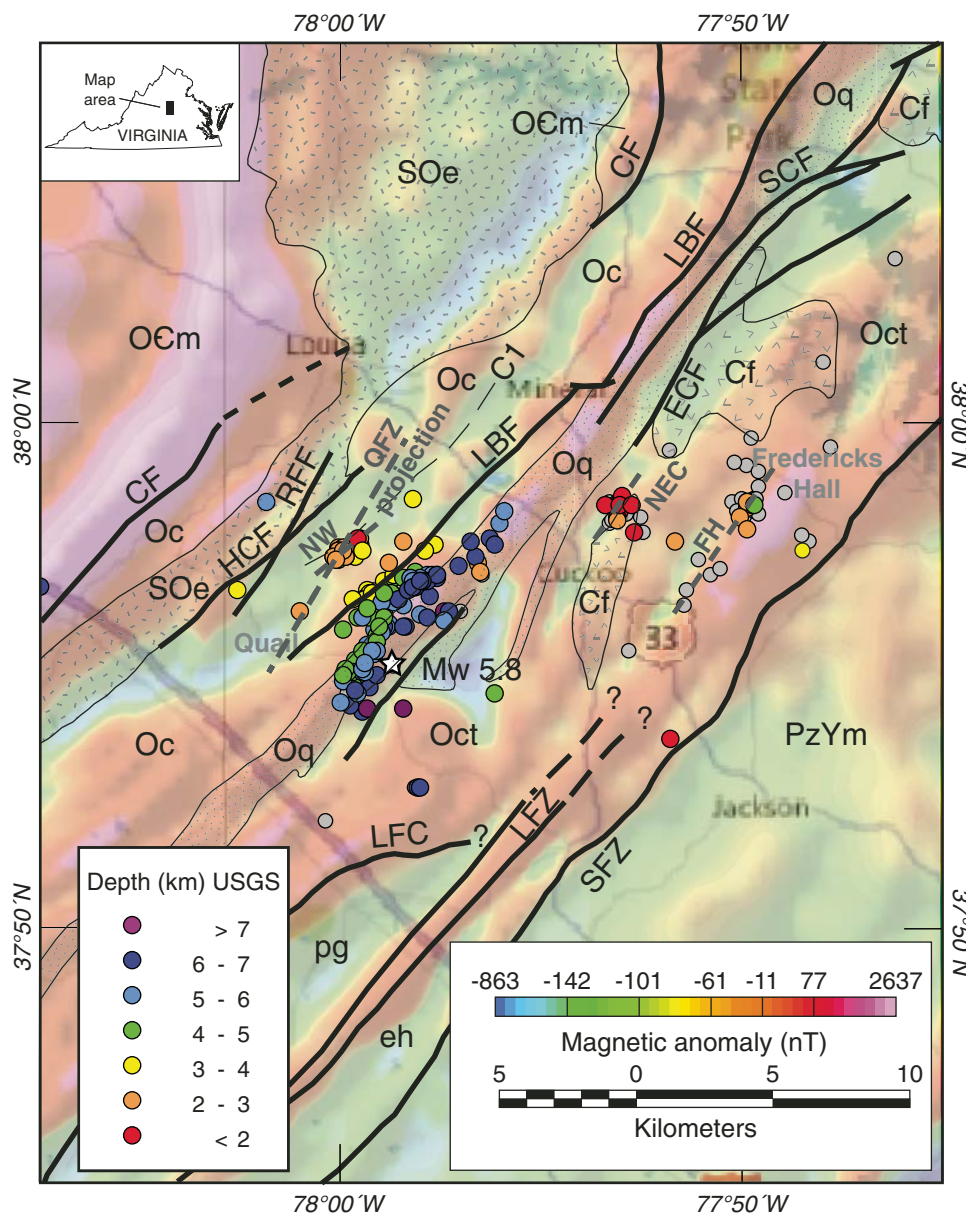


Figure 3. Relation of aftershock-illuminated faults to preexisting geologic structures including faults. Aeromagnetic map (color shaded relief) shows epicenters of aftershocks having magnitude $M \geq 2.0$, colored by depth where depth uncertainty is ≤ 1 km or gray where depth uncertainty is > 1 km, and aftershock-illuminated faults in relation to preexisting faults (solid black lines—previously mapped; dashed black lines—inferred projections). White star is M_w 5.8 mainshock epicenter. Aftershock-illuminated faults: QFZ—Quail fault zone, FH—Fredericks Hall fault, NW—northwest fault, NEC—fault northeast of Cuckoo. Preexisting (Paleozoic and Mesozoic) faults: CF—Chopawamsic fault, ECF—Ebenezer Church fault, HCF—Harris Creek fault at southeast contact of Ellisville Granodiorite pluton tail or neck (Burton et al., 2014, this volume), LBF—Long Branch fault zone, LFC—Little Fork Church fault, LFZ—Lakeside fault zone, RFF—Roundabout Farm fault, SCF—Sturgeon Creek fault, SFZ—Spotsylvania fault zone. Ordovician volcanic-arc sequences: Oc—Chopawamsic Formation, Oct—Chopawamsic Formation and Ta River Metamorphic Suite (undivided). Ordovician successor-basin deposits: Oq—Quantico Formation (mainly schist). Cambrian to Ordovician Potomac composite terrane: OEm—Mine Run Complex (mélanges). Mesoproterozoic–Paleozoic Goochland terrane: PzYm—Maidens gneiss and Po River Metamorphic Suite. Rocks of undetermined affinity: eh—Elk Hill Complex (undated metavolcanic; as used by Spears et al., 2004), pg—pegmatite-rich gneiss. Intrusive rocks: Cf—Carboniferous Falmouth Intrusive Suite (granite), SOe—Late Ordovician to early Silurian Ellisville Granodiorite pluton. Sources include citations in text, aeromagnetic data (from Snyder, 2005), and aftershock data (from McNamara et al., 2014a). C1—contact formerly mapped as Chopawamsic fault (e.g., Virginia Division of Mineral Resources, 1993; Marr, 2002).

ville Granodiorite pluton. Sources include citations in text, aeromagnetic data (from Snyder, 2005), and aftershock data (from McNamara et al., 2014a). C1—contact formerly mapped as Chopawamsic fault (e.g., Virginia Division of Mineral Resources, 1993; Marr, 2002).

(1978), Swanson (1986), and Withjack et al. (2012) for early Mesozoic brittle faults and rift basins; and Mixon et al. (2000, 2005) for Cretaceous and Cenozoic faults. The geologic setting of the aftershock cluster that defines the Quail fault zone is of special interest to determine if a preexisting Paleozoic, Mesozoic, or Cenozoic fault could have been reactivated.

Recent geologic mapping in the 2011 Mineral earthquake epicentral area (Hughes et al., 2013; Burton et al., 2014, this volume) indicates that an unusual ~1.5-km-wide southern tail or neck of the rheologically distinct Late Ordovician–early Silurian (443.7 ± 3.3 Ma, Hughes et al., 2013) Ellisville Granodiorite pluton (Fig. 3) is entirely within metavolcanic and metavolcaniclastic rocks of the Chopawamsic Formation, rather than cross-cutting the early Paleozoic Chopawamsic fault, as shown on previous reconnaissance maps (e.g., Virginia Division of Mineral Resources, 1993; Marr, 2002). Geologic mapping and trenching since the 2011 Mineral earthquake have also revealed the presence of two previously unknown faults, which are both characterized by Paleozoic ductile shear fabrics overprinted by late brittle structures: the Harris Creek fault (Fig. 3) strikes $\sim 044^\circ\text{--}050^\circ$ along and near the southeastern flank of the Ellisville pluton tail, whereas the Roundabout Farm fault strikes $\sim 025^\circ\text{--}030^\circ$ at an oblique angle to northeast-striking bedrock units and structures (Burton et al., 2014, this volume).

Vegetation and ground cover in the eastern United States obscure subtle features of the land surface that could potentially reveal surface expressions of Quaternary faults. Airborne laser swath mapping or LiDAR (light detection and ranging) is a promising new tool for locating and characterizing surface expressions of faults in forested and metropolitan areas (Sherrod et al., 2004; Engelkemeir and Khan, 2008). In March 2012 an airborne LiDAR survey was flown over a $\sim 20 \times 35$ km area covering the epicenters of the 23 August 2011 earthquake and most of its aftershocks. This survey produced an 8 points/m² LiDAR-derived bare earth digital elevation model. The LiDAR elevation data (1/9 arc-s) from this Louisa area survey are available from the USGS National Elevation Dataset at <http://viewer.nationalmap.gov/viewer/>.

Airborne geophysical surveys (radiometric, magnetic, and gravity) were flown in July 2012 with a trackline spacing of 200 m from a nominal height of 125 m with slightly greater heights over populated areas. Flight lines were oriented northwest-southeast, perpendicular to known structures. A 20×25 km area was covered, but the region over the town of Louisa was not flown due to flight altitude restrictions. Data and results from the magnetic and gravity surveys are discussed in Shah et al. (this volume), and those from the radiometric survey are considered herein. Airborne spectral radiometric (gamma-ray spectrometry) surveys map the estimated concentrations of radioactive elements (potassium, uranium, and thorium) within ~1 m of the land surface (Duval et al., 1971). Materials at this depth in the Virginia Piedmont are mainly residual soils that were locally derived from underlying bedrock.

Airborne gamma-ray spectrometry measures the gamma-ray flux caused by radioactive decay of potassium (K-40), uranium

(U-238), and thorium (Th-232). These data are used to estimate the apparent surface concentrations of potassium (K), uranium (U), and thorium (Th) as summarized in Duval (1983, and references therein). Uranium (eU) and thorium (eTh) symbols for measured gamma-ray fluxes are preceded by “e” for “equivalent” because they originate from daughter elements in the decay series. The radiometric (gamma-ray spectrometry) measurements were conducted using a Radiation Solutions RS-500 spectrometer system consisting of a NaI(Tl) detector volume of 58.8 L with 12 downward-looking and two upward-looking crystals of 4.2 L each. Data were collected in 1024 channel spectral models and windowed using an interval of 1 s. Stripping ratios were obtained using standard methods with calibration pads; thorium source tests were conducted at the start and end of each survey day. Cosmic and aircraft background corrections were estimated using standard methods on presurvey flight measurements at altitudes 1200–3000 m in Louisa County. Data were corrected for radon background radiation by using the upward-looking detectors. Absolute position of sensors was determined using a differential global positional system combined with radar altimeter and barometric data. Postprocessing included standard corrections for system dead time, drift, Compton scattering, height and attenuation, and microleveling for uranium measurements.

The LiDAR and radiometric data delineate subtle features of the land surface and the top meter or less of the Earth’s surface via relative amounts of potassium, uranium, and thorium. Radiometric potassium anomalies reflect the presence of potassium-bearing minerals such as muscovite or biotite mica and potassium feldspar.

Aftershock clusters delineate the active faults in this study, but did any of these faults reactivate preexisting structures? Radiometric anomalies that delineate preexisting units or structures based on their potassium, uranium, and thorium content are combined with LiDAR images of the land surface to address this question. Coincidence of preexisting structures with faults delineated by aftershocks can suggest that the structures were locally reactivated.

RESULTS

Aftershocks Illuminate the Quail Fault Zone and Other Faults

The majority of aftershock hypocenters, including those for some of the larger magnitude events (M_w 3.9, 3.8, and 3.2), are concentrated in a 10-km-long, 1-km-thick, northeast-striking, southeast-dipping tabular cluster that ranges in depth from ~3 to 8 km. This tabular cluster, which projects upward from beneath Yanceyville, Virginia, along the South Anna River toward Quail, Virginia (Figs. 2A, 2B, and 3), defines the previously unrecognized Quail fault zone (as used here and in Horton et al., 2012a, 2012b). The relocated main-shock hypocenter (Figs. 4A, 4B) is in the lower part of this cluster at ~6–8 km depth (7 ± 2 km; McNamara et al., 2014a; 8 ± 1 km; Chapman, 2013). Aftershocks within this cluster, including those having the larger magnitudes,

Aftershocks illuminate the 2011 Mineral, Virginia, earthquake causative fault zone

represent smaller fault ruptures that are mostly shallower than the main shock. Multiple fault strands that were active at different times are suggested by local planar concentrations of hypocenters within the main aftershock cluster (evident in 3D rotatable images; see footnote 1), and by evolution of the aftershock point cloud as observed in time-sequence animations (U.S. Geological Survey, 2012). The strike and dip of the Quail fault zone aftershock cluster ($036^\circ \pm 12^\circ$, $49.5^\circ \pm 6^\circ$ SE; 2σ ; McNamara et al., 2014a) and its early aftershocks (029° , 51° SE; Chapman, 2013) are consistent with the 028° , 50° SE main-shock nodal plane having mostly reverse slip. The 7° difference between early and later

aftershock-cluster strike angles, showing increasing deviation from RMT with time, is within the 2σ uncertainty. The subtle change in average strike angle as a function of time is consistent with concave-east curvature of the aftershock-delineated fault zone shown in the Appendix (C, D) and with later aftershocks (after October–November) that were slightly more abundant in the northeast part (Fig. 2B). The 029° strike of the southwestern part of this aftershock zone (D in Appendix) is essentially identical to that of the main-shock nodal plane and early aftershocks (Chapman, 2013), whereas the 047° strike of the northeastern part (C in Appendix), containing more abundant later

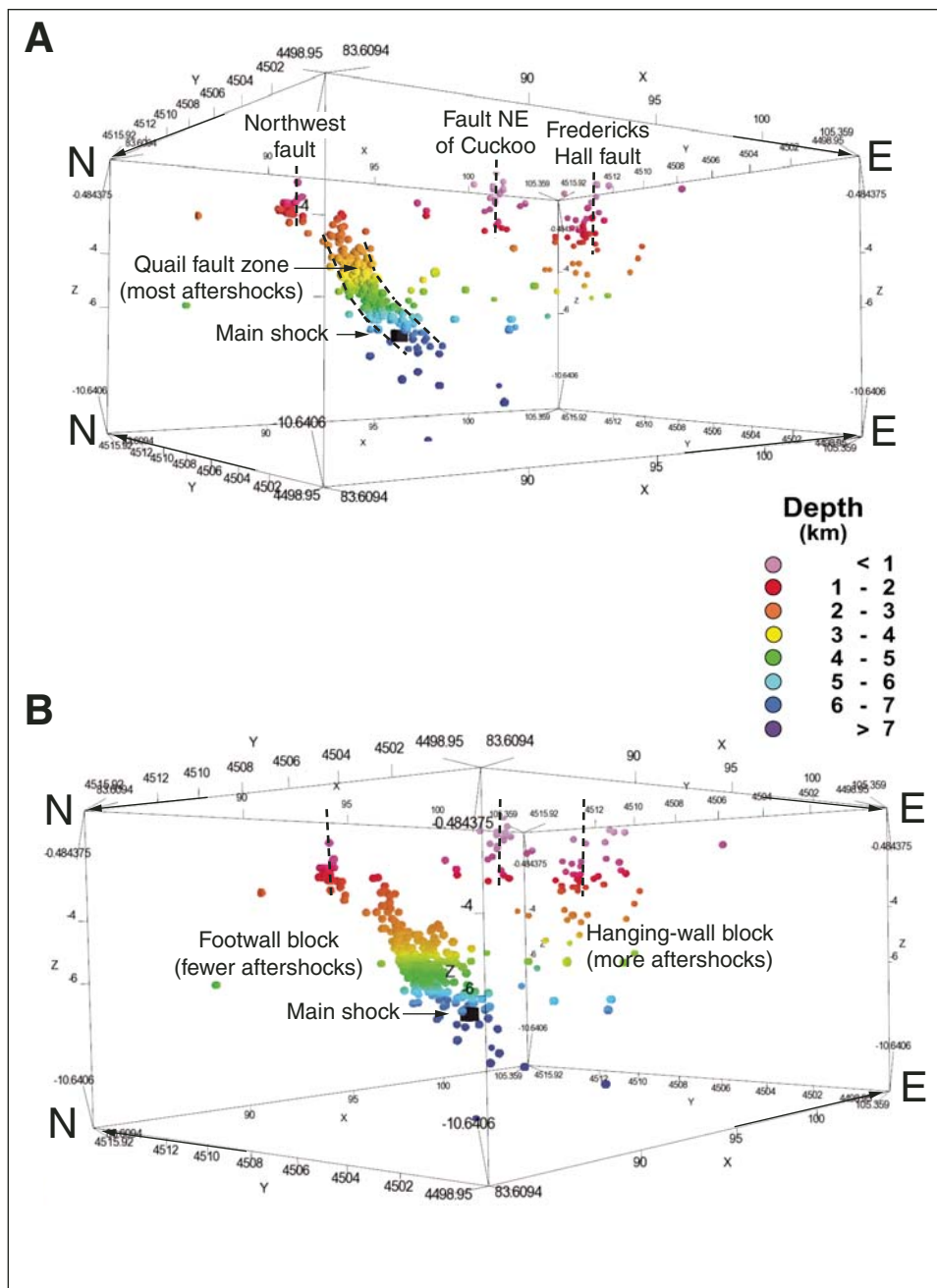


Figure 4. Aftershock and main-shock hypocenters (all hypocentroidal decomposition–relocated events) viewed in three dimensions. (A) Near-horizontal view looking $\sim 033^\circ$ along the strike of the Quail fault zone. (B) Near-horizontal view looking $\sim 045^\circ$ oblique to the main aftershock clusters. These views show the southeast-dipping Quail fault zone aftershock cluster, the relocated M_w 5.8 main shock near the base of this cluster, shallow aftershock clusters that illuminate subsidiary faults labeled in Figure 2, and the relative abundance of aftershocks in the hanging-wall block compared to the footwall block of the Quail fault zone. See related DR item R1 for fully rotatable 3D image (see footnote 1).

aftershocks, is closer to the local 040° – 050° strike of preexisting geologic units and structures. Quail fault zone aftershocks that were shallower than 4 km were also concentrated in the central and northern parts (Fig. 2A).

The following three clusters of more than 10 shallow aftershocks having depths <4.5 km (Figs. 2A, 2B) illuminate other active faults. (1) A linear cluster of early shallow aftershocks (mostly within 65 days) from August to October 2011 occurred ~ 10 km east of the main aftershock cluster that defines the Quail fault zone (Figs. 2A, 2B); this cluster extends ~ 8 km from Fredericks Hall, Virginia, to Threemile Corner, Virginia, strikes $\sim 035^{\circ}$ – 039° , and appears to be roughly vertical in 3D rotatable plots (DR item R1; see footnote 1). (2) A more prolonged cluster of shallow aftershocks (mostly within ~ 110 days) from September through December occurred 5–10 km northeast of the Quail fault zone aftershock cluster and is located ~ 3 km northeast of Cuckoo, Virginia (Figs. 2A, 2B). (3) A late northwest linear cluster of shallow aftershocks (mostly after 100 days and frequent for another 35 days) in December 2011 and January 2012 occurred ~ 1 km northwest of the Quail fault zone aftershock cluster (Figs. 2A, 2B). Visual examination of cross sections (Fig. 2C), and 3D views (Figs. 4A, 4B) and rotatable plots (e.g., DR item R1; see footnote 1) suggests that the late northwest cluster has a more eastward strike and steeper (near vertical?) dip than the larger Quail fault zone cluster.

Tectonic Relations of the Quail Fault Zone

The Quail fault zone (Fig. 3) aftershock cluster, when projected to the surface, is within Chopawamsic Formation gneiss, which is locally mylonitic, near or just southeast of the $\sim 050^{\circ}$ trending tail of the Ellisville Granodiorite pluton (Horton et al., 2012b). The 028° striking main-shock nodal plane of the Mineral earthquake (Herrmann, 2011) and the 029° striking early aftershocks in the Quail fault zone cluster (Chapman, 2013) are oblique to the northeastern strikes of most geologic map units in this area, and they are also oblique to the $\sim 044^{\circ}$ – 050° striking Harris Creek fault (Fig. 3) as mapped by Burton et al. (2014, this volume). However, they are essentially parallel to the $\sim 025^{\circ}$ – 030° striking Roundabout Farm fault (Fig. 3) of Burton et al. (2014, this volume). Further investigations may determine if seismic activity on the Quail fault zone is causally related to a preexisting fault such as the Roundabout Farm fault.

The deep southeast end of the Quail fault zone aftershock cluster terminates beneath the surface trace of moderately to steeply southeast-dipping schist of the Ordovician Quantico Formation and associated faults, including the Long Branch fault zone (Fig. 3). The Quail fault zone and main-shock epicenter also coincide with a gentle convex-east bend of $\sim 15^{\circ}$ in the strike of bedrock geologic units (e.g., 048° to 033° for the northwest contact of the Quantico Formation; Fig. 5) as well as trends of associated topographic features and geophysical anomalies (Shah et al., 2012b, this volume). Strikes of 030° – 040° northeast of the main-shock epicenter rotate to 040° – 050° southwest of it. The strikes of bedrock units to the northeast more closely approximate azimuths of the main-shock nodal

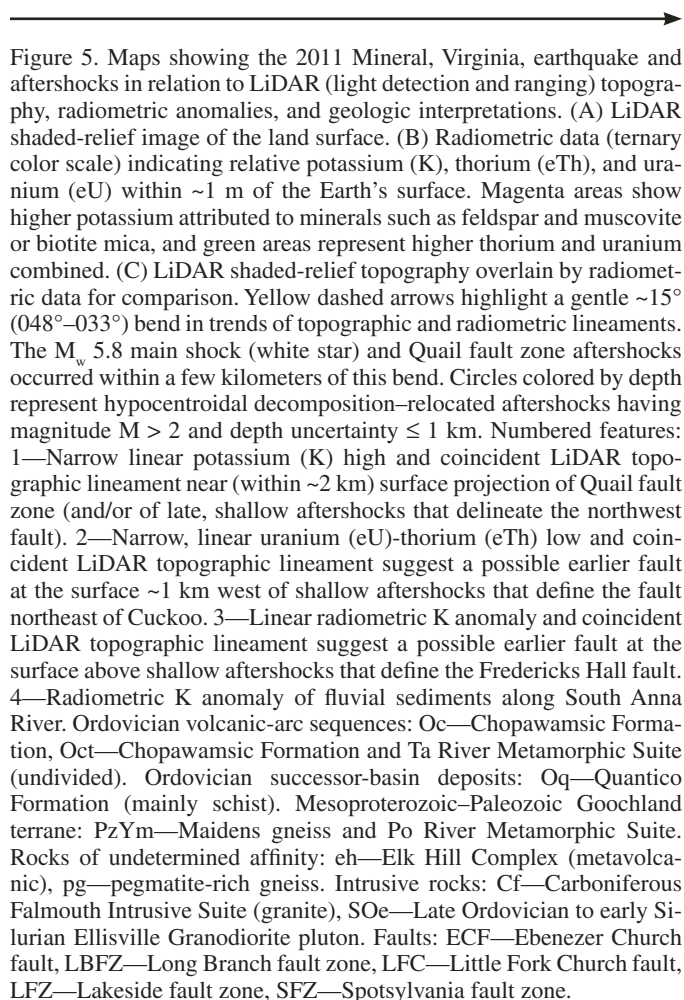
plane, and of the Quail fault zone as delineated by aftershocks, than those to the southwest in the vicinity of the Interstate Highway I-64 seismic profile.

Tectonic Relations of Other Aftershock-Illuminated Faults

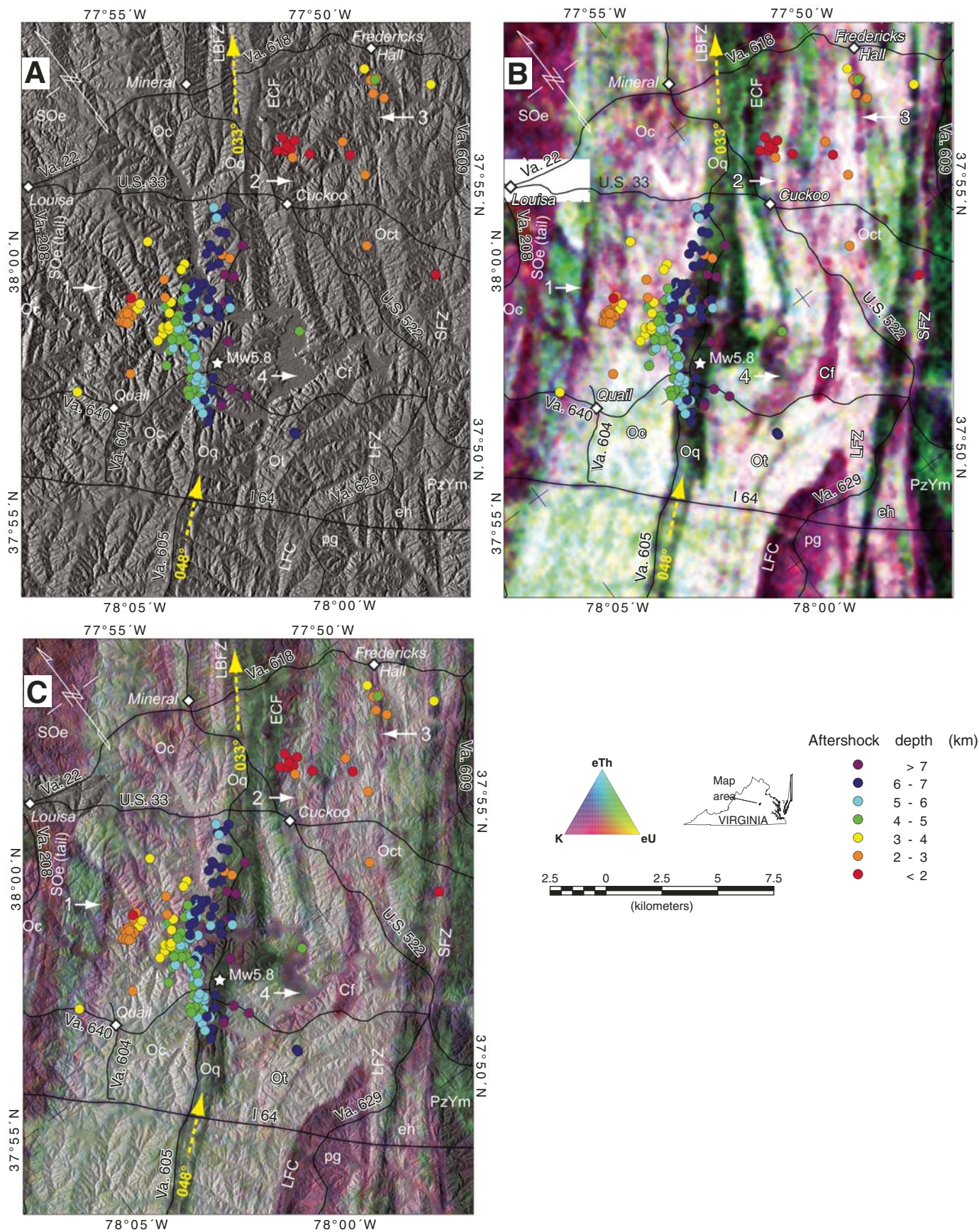
Some of the outlying aftershock clusters that represent active faults appear to have spatial associations with preexisting geologic features including faults (Fig. 3). Such associations might suggest reactivation or strain localization.

Fault Northeast of Cuckoo

Several kilometers east of the Quail fault cluster, a tight cluster of ~ 10 hypocenters <3 km deep is located ~ 3 km northeast of Cuckoo (Fig. 2). This cluster of shallow aftershocks, described as the fault northeast of Cuckoo, is ≤ 2 km southeast of a moderately to steeply dipping Paleozoic fault, here termed the Ebenezer Church fault (Fig. 3), which was mapped by Mixon et al. (2000) along the southeastern contact of the Quantico Formation. Geologic mapping in progress (Burton et al., 2014, this volume) indicates the presence of faults near the same Quantico



Aftershocks illuminate the 2011 Mineral, Virginia, earthquake causative fault zone



Formation contact several kilometers southwest of the aftershock cluster. If one hypothetically assumes a southeast dip, then the aftershock-illuminated fault northeast of Cuckoo (Fig. 3) would project to the surface at or just southeast of the southeastern contact of the Quantico Formation (Fig. 3). Alternatively, a steeper surface projection could coincide with a $\sim 033^\circ$ trending LiDAR topographic lineament and linear radiometric anomaly shown as feature 2 in Figure 5. A single RMT solution from this aftershock cluster (Fig. 2C) is anomalous relative to all the others, possibly reflecting the orientation of preexisting structures or reorientation of the regional stress field following the main shock, as well as the shallow depth.

Fredericks Hall Fault

Approximately 10 km east of the Quail fault zone aftershock cluster, an elongate cluster of 12–13 early aftershocks near Fredericks Hall spans a lateral distance of ~ 8 km. This aftershock cluster delineates the Fredericks Hall fault (as used here and in Horton et al., 2012a, 2012b). The Fredericks Hall fault strikes $\sim 035^\circ$ – 039° , based on the alignment of aftershocks (Figs. 2A, 2B, and 3), and a near vertical dip is roughly suggested by visual examination of 3D rotatable plots (DR item R1; see footnote 1). The best-located aftershocks (having depth uncertainties ≤ 1 km) in this cluster have shallow depths of $< \sim 4.5$ km (Fig. 2B). The surface projection of this fault, assuming a near vertical dip, coincides with a $\sim 033^\circ$ – 036° trending LiDAR topographic lineament and linear radiometric potassium high anomaly shown as feature 3 in Figure 5. The latter features indicate a preexisting structure (perhaps another shear zone containing muscovite, as confirmed at feature 1 in Fig. 5) at the location of the aftershock-delineated Fredericks Hall fault. Linear magnetic anomalies suggest that the Fredericks Hall fault (as used here and in Horton et al., 2012a, 2012b), may extend more than 20 km southward to form the southeastern boundary of pegmatite-rich gneiss (Figs. 3 and 5). The Lakeside fault zone forms the southeastern boundary of this pegmatite-rich gneiss near Interstate Highway I-64 (Spears et al., 2004), spans a width of several kilometers (Bourland et al., 1979), and bounds the early Mesozoic Farmville rift basin (Wilkes, 1982), as shown in Figure 1. Spears (2011) reported a Jurassic diabase dike offset on the Lakeside fault just south of the James River. Further geologic mapping may determine whether the Fredericks Hall fault represents a reactivated strand or splay of the Lakeside fault zone shown in Figures 3 and 5.

Northwest Fault

An elongate cluster of late shallow aftershocks ~ 1 km northwest of the main Quail fault zone aftershock cluster delineates the northwest fault (Fig. 3; as described here and in Horton et al., 2012a, 2012b), which is spatially and temporally distinct, dips more steeply, and has a more northeastward strike. The cluster consists of > 10 late (December 2011 to January 2012) aftershocks $< \sim 4$ km in depth. Aftershocks associated with the northwest fault cluster near an updip projection of the Quail fault zone but are separated by an ~ 1 km gap (Fig. 2B). Visual examination of maps and cross sections (Fig. 2), 3D views (Figs. 4A, 4B) and rotatable plots (e.g., DR item

R1; see footnote 1) suggests that the late northwest cluster has a more eastward strike and steeper (near vertical?) dip than the main Quail fault zone cluster.

Aftershock clusters associated with both the northwest fault and with the Quail fault zone could project to the surface in the vicinity of Harris Creek, where ductile and brittle structures suggest a history of repeated faulting (Burton et al., 2014, this volume). If late, shallow aftershocks of the northwest fault cluster represent an outlying strand of the Quail fault zone dipping $\sim 45^\circ$ SE (rather than a steeper fault as suggested herein), then its surface projection would coincide approximately with the $\sim 045^\circ$ trending LiDAR topographic lineament and linear radiometric K anomaly shown as feature 1 in Figure 5 and the associated $\sim 044^\circ$ – 050° striking Harris Creek fault (HCF in Fig. 3), where Burton et al. (2014) reported secondary growth of muscovite along S_2 foliation in shear zones. These relations suggest that localization of late seismicity on the northwest fault may have been influenced by reactivation of the Harris Creek fault, or possibly by rheological contrast between the Ellisville Granodiorite tail and more friable gneiss of the Chopawamsic Formation.

Spotsylvania Fault Zone

East of the shallow aftershock clusters mentioned, sparse aftershocks near the Spotsylvania fault zone show no alignment or clustering that would suggest reactivation following the Mineral earthquake (Figs. 3 and 5). The lack of spatial association between the aftershock sequence and this Paleozoic terrane-bounding fault, which also underlies Cretaceous and Cenozoic reverse faults of the Stafford fault system to the northeast in the coastal plain (Mixon et al., 2000, 2005), is noteworthy. Major Paleozoic faults such as the Spotsylvania zone formed when rocks currently on the surface were at mid-crustal levels, when strain rates were many times greater than now, and when stress fields had different orientations. The lack of spatial correlation with earthquakes suggests that the Spotsylvania zone is not oriented favorably to have high resolved shear stress in the present stress regime, perhaps because of the gentle dip angles indicated by seismic reflection (e.g., Pratt et al., this volume).

DISCUSSION

Although many faults have been mapped in the Central Virginia seismic zone, none of the previously mapped faults clearly correspond to the 2011 Mineral earthquake or previous earthquakes (Fig. 1). Well-located aftershocks in this study show no seismic activity on early Paleozoic thrusts such as the terrane-bounding Chopawamsic fault and little if any activity on the terrane-bounding late Paleozoic Spotsylvania fault zone. The presence of mapped faults in this passive-margin seismic zone does not imply that they will be active, and experience in the region suggests that many faults have yet to be mapped. This study of aftershock-illuminated faults in a passive-margin setting suggests more subtle relations between earthquakes and preexisting geology.

Aftershocks illuminate the 2011 Mineral, Virginia, earthquake causative fault zone

Early Mesozoic rift basins are present within the Central Virginia seismic zone but are outside the geographic range of the Mineral earthquake and its aftershocks, although the Lakeside and Spotsylvania fault zones extend from the epicentral area to the early Mesozoic Farmville basin (Fig. 1). However, possible offset of a Jurassic diabase dike along the Harris Creek fault (Burton et al., 2014, this volume) is consistent with the concept that passive-margin seismicity in the eastern United States can be locally influenced by reactivation of rift-related extensional faults that preceded opening of the Atlantic Ocean.

The occurrence of the 2011 Mineral earthquake on a northeast-striking reverse fault is consistent with east-southeast-trending (102° ; Herrmann, 2011) to southeast-trending (133° ; Kim and Chapman, 2005) maximum horizontal compressive stresses in the Central Virginia seismic zone, rather than northeast-southwest compressive stresses that characterize most of eastern North America (Zoback, 1992; Mazzotti and Townend, 2010). The 7 ± 2 km depth of the 23 August 2011 earthquake is near the mean depth for previous earthquakes in the Central Virginia seismic zone (Chapman, 2013). The scattered locations of historical and recent earthquakes within this zone indicate that these earthquakes occurred on different faults within thrust sheets interpreted from packages of seismic reflectors (Bollinger and Sibol, 1985; Munsey and Bollinger, 1985; Çoruh et al., 1988; Pratt et al., 1988, this volume; Kim and Chapman, 2005). This scattered distribution of earthquakes in the Central Virginia seismic zone differs in character from the New Madrid seismic zone, where earthquakes are localized on a few well-defined faults (e.g., Pratt, 2012).

Most of the moment release from the main shock occurred in a small area of 2–3 km radius at ~6–8 km depth (Chapman, 2013). A broadside cross-sectional view of the main aftershock cluster (Fig. 2D), 3D view (Fig. 4B), and rotatable plot (DR item R1; see footnote 1) show a rough semicircular distribution of aftershocks in the Quail fault zone cluster above and to the northeast of this area that underwent most of the main-shock slip. This observation suggests that, after removal of crustal stress by the main shock in the area of maximum slip and stress drop, aftershocks were concentrated in portions of the fault zone where stress was transferred and increased (McNamara et al., 2014a).

The 23 August 2011 main-shock hypocenter in the Quail fault zone is ~6 km northeast of a 1981 USGS seismic-reflection profile along Interstate Highway I-64 (Harris et al., 1982). Seismic images along the I-64 profile are interpreted to indicate that the earthquake occurred within thrust sheets that were emplaced westward over Laurentian (ancestral North American) crust of Mesoproterozoic age (Harris et al., 1982, 1986; Pratt et al., 1988, this volume), although rock structures in the Piedmont Province indicate that ductile transpressive strains are dominant (Bailey et al., 2004). The hypocenter is beneath surface exposures of the Chopawamsic terrane, which was a magmatic arc sequence that accreted to the Laurentian continent during the Late Ordovician between ca. 453 and 444 Ma (Hughes et al., 2013). Reprocessing of the I-64 profile data (Pratt et al., this volume) indicates that the Chopawamsic terrane is composed of relatively thin (≤ 4.5 km),

gently dipping reflector packages interpreted to represent thrust sheets. Following the 7 ± 2 km deep main shock, seismic activity in the Quail fault zone propagated across these gently dipping reflectors, interpreted to represent thrust sheets, as small fault ruptures in the steeper southeast-dipping aftershock zone to depths of 3–4 km. The ~7 km focal depth is within or above an ~2-km-thick highly reflective zone defined by discontinuous reflections, but without offset that would be expected for a steeper, crosscutting fault of resolvable displacement (Pratt et al., this volume).

The Mineral earthquake occurred near a gentle bend in the regional strike of geologic units such as the Quantico Formation and structures such as the Long Branch fault zone, and this bend is also reflected in topographic and geophysical lineaments (Figs. 3 and 5). These features trend $\sim 033^\circ$ to the northeast of the bend, where they are continuous for ~50 km toward Washington, D.C., and trend $\sim 048^\circ$ to the southwest of the bend (Fig. 5), where they appear to be continuous for ~20 km. This gentle bend in strike of bedrock units at the Mineral earthquake epicenter and Quail fault zone aftershock cluster suggests that, if dip angles are relatively constant, a contrast in resolved shear stress on preexisting fault segments at different angles to the maximum compressive stress northeast and southwest of this bend could have influenced the earthquake location. Local perturbation of the stress field at the bend in strike between these differently oriented segments having slightly different shear-stress components may have provided a trigger point for initial seismic moment release in the Mineral earthquake. Regional magnetic and gravity anomalies that have been filtered to reflect geologic sources at different depths show the same bend and suggest a similar interpretation (Shah et al., this volume).

The strike of the Quail fault zone aftershock cluster bends from $\sim 029^\circ$ in the southwestern part, where it closely approximates strikes of the main-shock nodal plane and cluster of early aftershocks (Chapman, 2013), to $\sim 047^\circ$ in the northeastern part (Appendix), where it is closer to the local 040° – 050° strike of host-rock geologic units. This concave-east bend in strike of the Quail fault zone aftershock cluster and concentration of aftershocks shallower than 4 km in the northeastern part suggest slight differences in seismic response for these two parts of the fault zone. The main shock (including three subevents of Chapman, 2013) and majority of early aftershocks were deeper than ~4 km and concentrated in the southwestern part, whereas the December 2011 and later aftershocks were mostly shallower than ~4 km and more abundant in the northeastern part. These relations suggest that the influence of preexisting structures on aftershock patterns increased with time, and with distance northeast of the main shock.

Chapman (2013) determined that the main-shock rupture occurred slightly beneath the plane defined by early aftershock hypocenters, possibly on a slightly deeper parallel fault. If so, then the main aftershock zone could represent smaller fault ruptures in the main-shock hanging-wall block. Farther away, most outlying aftershocks beyond the main cluster, including those associated with the Fredericks Hall fault and the fault northeast of Cuckoo, are in the hanging-wall block of the southeast-dipping Quail fault zone. These relations are consistent with interpretations based on

aftershock-distribution observations from the 1994 Northridge and 2003 San Simeon earthquakes in California, and the 2008 Wenchuan earthquake in Sichuan, China. In some segments of the causative faults responsible for these reverse-fault, main-shock earthquakes, aftershocks were found to be concentrated along the rupture plane and in the hanging-wall block, whereas aftershocks in the footwall block were less common (Shearer et al., 2003; McLaren et al., 2008; Zhang et al., 2010).

Three of the aftershock-illuminated faults identified in this study are associated with linear radiometric potassium anomalies and coincident LiDAR lineaments that are interpreted to represent preexisting potassium-bearing units or structures (Fig. 5). At least one of these anomalies (feature 1 in Fig. 5) represents muscovite that formed along the Harris Creek fault (W. Burton, 2013, oral commun.). These observations suggest that some ruptures during the 2011 Mineral earthquake and aftershock sequence occurred along preexisting faults and/or were influenced by preexisting geologic material contrasts, whereas other faults (e.g., Spotsylvania zone) were inactive in the regional stress field. The Harris Creek fault (Fig. 3) coincides with a geologic contact between the rheologically distinct Ordovician–Silurian Ellisville Granodiorite and more friable gneiss of the Ordovician Chopawamsic Formation, and shows evidence of repeated Paleozoic to Cenozoic faulting (Burton et al., 2014, this volume).

Aftershocks deeper than ~3.5 km are concentrated in the main aftershock cluster that defines the Quail fault zone, whereas shallower aftershocks are widely dispersed, mostly in the main-shock hanging-wall block, and include the smaller clusters that illuminate subsidiary faults. Although not precisely determined, strikes and dips of some shallow aftershock clusters resemble those of preexisting faults, foliations, and geologic contacts. If late shallow aftershocks of the northwest fault cluster are interpreted as an outlier of the larger Quail fault zone dipping ~45°SE, then this smaller cluster can be projected to the surface along a linear radiometric potassium anomaly and LiDAR topographic lineament (feature 1 in Fig. 5) at the Harris Creek fault (Fig. 3) of Burton et al. (2014, this volume). Aftershocks that illuminate the fault northeast of Cuckoo are tightly clustered, but assuming a southeast dip, can be projected to the surface at or just southeast of the Quantico Formation, where preexisting faults have been mapped to the northeast and southwest.

The linear aftershock cluster that illuminates the Fredericks Hall fault has a strike of ~035°–039° and appears to be approximately vertical. Alignment of these shallow aftershocks along a linear radiometric potassium anomaly and parallel LiDAR lineament (feature 3 in Fig. 5) indicates that the aftershock fault ruptures occurred on a preexisting geologic unit or structure. Linear magnetic anomalies suggest that the Fredericks Hall fault extends more than 20 km southwest to form the southeastern boundary of pegmatite-rich gneiss (Figs. 3 and 5). Thus, the Fredericks Hall fault may represent a western strand or splay of the Lakeside fault zone, which to the south spans a width of several kilometers (Bourland et al., 1979) and bounds the western edge of the early Mesozoic Farmville basin (Figs. 1, 3, and 5).

Aftershock occurrences along strands or splays of preexisting faults with considerable length would suggest that earthquakes larger than M_w 5.8 are possible in the Central Virginia seismic zone. This conclusion is consistent with paleoliquefaction evidence for Holocene seismic activity (Obermeier and McNulty, 1998; Schindler et al., 2012). However, lengths of aftershock clusters on faults may be more closely related to moment release than mapped fault lengths (Wells and Coppersmith, 1994; Leonard, 2010).

CONCLUSIONS

Aftershock hypocenters of the 23 August 2011, Mineral, Virginia, earthquake sequence image the causative fault of a significant earthquake for the first time in the Central Virginia seismic zone. The majority of aftershocks, including several of the larger ones, delineate the southeast-dipping Quail fault zone in which the main shock occurred in the lower part. Most of the aftershocks that have well-determined focal mechanisms are within this zone and have an approximately parallel nodal plane.

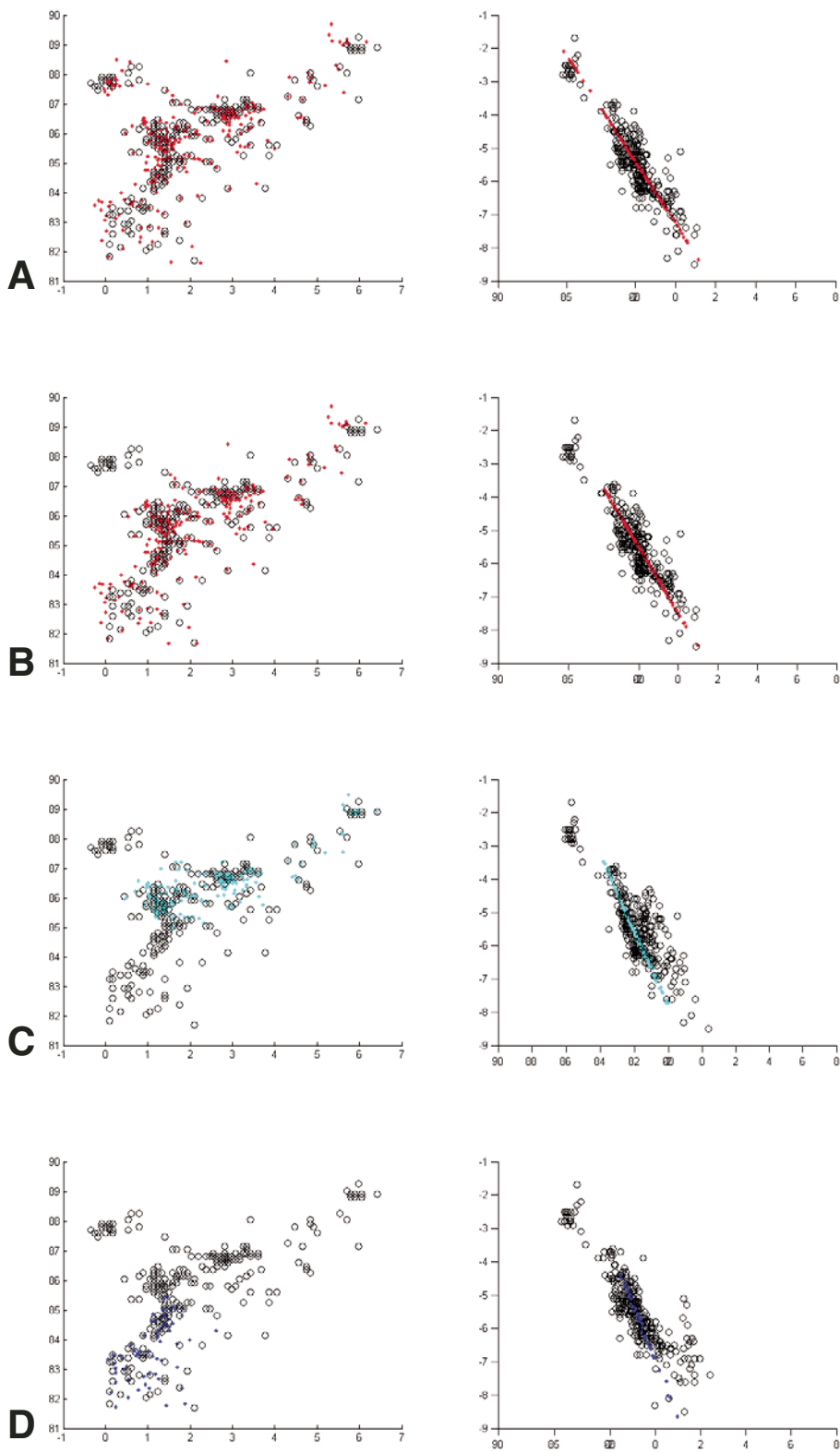
The nature and scope of intraplate earthquake hazards associated with the Central Virginia seismic zone and similar zones in eastern North America remain poorly understood. Nevertheless, the fault parameters determined in this study contribute to an improved understanding of earthquakes in the region. Historical seismicity in the Central Virginia seismic zone appears to involve widely scattered faults of small displacement. However, preexisting geology, including older faults, likely influenced the locations of the 23 August 2011 earthquake and the locations of some aftershocks. The 2011 Mineral, Virginia, earthquake and aftershocks on the previously unknown Quail fault zone project to the surface near the southeastern contact of the Ordovician–Silurian Ellisville Granodiorite pluton tail (or neck) with gneiss of the Ordovician Chopawamsic Formation. This contact has a northeast strike and southeast dip (similar to that of the Quail fault zone), and ongoing field studies indicate repeated Paleozoic to Cenozoic fault deformation in the area (Burton et al., 2014, this volume).

The 2011 Mineral earthquake occurred near a slight bend in strike of geologic units (Fig. 5). This association suggests that, if dip angles are relatively constant, preexisting fault segments having slightly different resolved shear-stress could have provided a trigger point for the seismic moment release. The evidence for clusters of aftershocks on preexisting geologic features identified by linear radiometric potassium anomalies, including the Harris Creek fault, further suggests that optimally oriented preexisting structures, locally modified stresses, and/or local rheological strength contrasts could have contributed to the locations of the earthquake and aftershocks.

In terms of known Paleozoic terrane-bounding faults in the vicinity of the Mineral earthquake aftershock sequence, the Spotsylvania fault zone shows little if any activity, and the Chopawamsic fault shows none. However, more detailed geologic mapping is needed to determine if the Fredericks Hall fault, as illuminated by shallow aftershocks, represents an active western strand or splay of the Lakeside fault zone, which to the south spans a width of several kilometers and bounds the Mesozoic Farmville rift basin.

Aftershocks illuminate the 2011 Mineral, Virginia, earthquake causative fault zone

APPENDIX. BEST-FIT PLANES FOR MAIN AFTERSHOCK CLUSTER (QUAIL FAULT ZONE)



Best-fit planes to HD aftershock data were calculated using a principal component analysis algorithm in Matlab (www.mathworks.com). Circles represent events and dots represent their projections to the best-fit plane. Left images show plan view; right images show the down-dip vertical cross section. Axis units show projected coordinates in km (a local Mercator projection was used). For vertical slices, which are oblique to the east-west and north-south axes, the axes can be distinguished by their ranges. East-west coordinates range from -1 to 7 km, and north-south coordinates range from 81 to 90 km. Root mean squared error (RMSE) includes a term for number of observations; note the decrease in RMSE for the split between two planes designated plane 1 (northeast part) and plane 2 (southwest part). (A) All events including shallow northwest cluster: strike = 34.8368 , dip = 48.4005 , RMSE = 0.35455 , mean of residuals = 0.16879 , 0.11747 . (B) All events excluding shallow northwest cluster: strike = 35.2969 , dip = 50.7036 , RMSE = 0.3558 , mean of residuals = 0.17456 , 0.12358 . (C) Northeast part (plane 1): strike = 47.047 , dip = 58.6837 , RMSE = 0.2731 , mean of residuals = 0.12483 , 0.13408 , 0.11145 . (D) Southwest part (plane 2): strike = 29.4264 , dip = 61.5795 , RMSE = 0.228 , mean of residuals = 0.13727 , 0.077433 , 0.085291 .

ACKNOWLEDGMENTS

We appreciate the rapid response of aftershock-deployment field crews from multiple institutions, including the U.S. Geological Survey, Virginia Polytechnic Institute and State University (Blacksburg), Lamont-Doherty Earth Observatory of Columbia University (New York), University of Memphis Center for Earthquake Research and Information (Tennessee), Lehigh University (Bethlehem, Pennsylvania), Incorporated Research Institutions for Seismology (IRIS), and Cornell University (Ithaca, New York). We also thank reviewers Christopher Bailey, William Burton, Ariel Conn, David Spears, Mark Steltenpohl, Christopher Swezey, and Lisa Walsh as well as volume editor Martin Chapman for constructive comments and suggestions that significantly improved the manuscript. The paper also benefitted from informal discussions with colleagues, including Mark Carter, Nick Evans, Amy Gilmer, Richard Harrison, Robert Herrmann, James Hibbard, Stephen Hughes, Thomas Pratt, and Robert Williams. Any use of trade, product, or firm names is for descriptive purposes only and does not imply endorsement by the U.S. government. This is U.S. Geological Survey manuscript IP-053749.

REFERENCES CITED

- Algermissen, S.T., and Perkins, D.M., 1976, A probabilistic estimate of maximum acceleration in rock in the contiguous United States: U.S. Geological Survey Open-File Report 76-416, 45 p.
- Bailey, C.M., 2004, Shaken! Earthquake rocks central Virginia, *in* The Geology of Virginia: Williamsburg, Virginia, College of William and Mary, 3 p., http://web.wm.edu/geology/virginia/whats_new/QuakeStory.pdf?svr=www (May 2013).
- Bailey, C.M., and Owens, B.E., 2012, Traversing suspect terranes in the central Virginia Piedmont: From Proterozoic anorthosites to modern earthquakes, *in* Eppes, M.C., and Bartholomew, M.J., eds., From the Blue Ridge to the Coastal Plain: Field Excursions in the Southeastern United States: Geological Society of America Field Guide 29, p. 327–344, doi:10.1130/2012.0029(10).
- Bailey, C.M., Francis, B.E., and Fahrney, E.E., 2004, Strain and vorticity analysis of transpressional high-strain zones from the Virginia Piedmont, USA, *in* Alsop, G.I., Holdsworth, R.E., McCaffrey, K.J.W., and Hand, M., eds., Flow Processes in Faults and Shear Zones: Geological Society of London Special Publication 224, p. 249–264, doi:10.1144/GSL.SP.2004.224.01.16.
- Bobyarchick, A.R., and Glover, L., III, 1979, Deformation and metamorphism in the Hylas zone and adjacent parts of the eastern Piedmont in Virginia: Geological Society of America Bulletin, v. 90, Part 1, p. 739–752, doi:10.1130/0016-7606(1979)90<739:DAMITH>2.0.CO;2.
- Bollinger, G.A., and Hopper, M.G., 1971, Virginia's two largest earthquakes—December 22, 1875, and May 31, 1897: Seismological Society of America Bulletin, v. 61, p. 1033–1039.
- Bollinger, G.A., and Sibol, M.S., 1985, Seismicity, seismic reflection studies, gravity and geology of the central Virginia seismic zone: Part I. seismicity: Geological Society of America Bulletin, v. 96, p. 49–57, doi:10.1130/0016-7606(1985)96<49:SSRSGA>2.0.CO;2.
- Bourland, W.C., Glover, L., III, and Poland, F.B., 1979, Lakeside fault zone, *in* Glover, L., III, and Tucker, R.D., eds., Field trip 1. Virginia Piedmont geology along the James River from Richmond to the Blue Ridge, *in* Guides to Field Trips 1–3 for Southeastern Section Meeting, Geological Society of America: Blacksburg, Virginia Polytechnic Institute and State University, p. 17–18.
- Bradley, D.C., 2008, Passive margins through earth history: Earth-Science Reviews, v. 91, p. 1–26, doi:10.1016/j.earscirev.2008.08.001.
- Brown, L., Quiros, D., Davenport, K., Hole, J., Han, L., Chen, C., and Mooney, W., 2012, Aftershock imaging with dense arrays (AIDA): 3D reflection imaging of local structure using aftershock sources recorded by dense deployment of earthscope portable instruments following the August 23, 2011, M_w 5.8, Virginia earthquake: Geological Society of America Abstracts with Programs, v. 44, no. 7, p. 382.
- Burton, W.C., Spears, D.B., Harrison, R.W., Evans, N.H., Schindler, J.S., and Counts, R., 2014, Geology and neotectonism in the epicentral area of the 2011 M_w 5.8 Mineral, Virginia, earthquake, *in* Bailey, C.M., and Coiner, L.V., eds., Elevating Geoscience in the Southeastern United States: New Ideas about Old Terranes: Field Guides for the GSA Southeastern Section Meeting, Blacksburg, Virginia, 2014: Geological Society of America Field Guide 35, p. 103–127, doi:10.1130/2014.0035(04).
- Burton, W.C., Harrison, R.W., Spears, D.B., Evans, N.H., and Mahan, S.A., 2015, this volume, Geologic framework and evidence for neotectonism in the epicentral area of the 2011 Mineral, Virginia, earthquake, *in* Horton, J.W., Jr., Chapman, M.C., and Green, R.A., eds., The 2011 Mineral, Virginia, Earthquake and its Significance for Seismic Hazards in Eastern North America: Geological Society of America Special Paper 509, doi:10.1130/2015.2509(20).
- Calais, E., Freed, A.M., Van Arsdale, R., and Stein, S., 2010, Triggering of New Madrid seismicity by late-Pleistocene erosion: Nature, v. 466, no. 7306, p. 608–611, doi:10.1038/nature09258.
- Chapman, M.C., 2013, On the rupture process of the 23 August 2011 Virginia earthquake: Seismological Society of America Bulletin, v. 103, p. 613–628, doi:10.1785/0120120229.
- Chapman, M.C., Mathena, E.C., and Snoke, J.A., 2006, Southeastern United States Seismic Network Bulletin, Number 40, January 1, 2005–December 31, 2005: Blacksburg, Department of Geosciences, Virginia Polytechnic Institute and State University, 36 p.
- Çoruh, C., Bollinger, G.A., and Costain, J.K., 1988, Seismogenic structures in the central Virginia seismic zone: Geology, v. 16, p. 748–751, doi:10.1130/0091-7613(1988)016<0748:SSITCV>2.3.CO;2.
- Duval, J.S., 1983, Composite color images of aerial gamma-ray spectrometric data: Geophysics, v. 48, p. 722–735.
- Duval, J.S., Cook, B., and Adams, J.A.S., 1971, A study of the circle of investigation of an airborne gamma-ray spectrometer: Journal of Geophysical Research, v. 76, p. 8466–8470, doi:10.1029/JB076i035p08466.
- Earthquake Engineering Research Institute, 2011, Learning from Earthquakes, The M_w 5.8 Virginia Earthquake of August 23, 2011: EERI Special Earthquake Report, December 2011, 13 p., <http://www.eqclearinghouse.org/2011-08-23-virginia/files/2011/12/EERI-GEER-DRC-Virginia-eq-report.pdf> (January 2012).
- Ellsworth, W.L., Imanishi, K., Luetgert, J.H., Kruger, J., and Hamilton, J., 2011, The M_w 5.8 Virginia earthquake of August 23, 2011 and its aftershocks: A shallow high stress drop event [abs.]: American Geophysical Union, 2011 Fall Meeting, abs. S14B-05, <http://static.coreapps.net/agu2011/html/S14B-05.html> (May 2013).
- Engelkemeir, R.M., and Khan, S.D., 2008, Lidar mapping of faults in Houston, Texas, USA: Geosphere, v. 4, p. 170–182, doi:10.1130/GES00096.1.
- Farrar, S.S., 1984, The Goochland granulite terrane: Remobilized Grenville basement in the eastern Virginia Piedmont, *in* Bartholomew, M.J., ed., The Grenville Event in the Appalachians and Related Topics: Geological Society of America Special Paper 194, p. 215–228, doi:10.1130/SPE194-p215.
- Gates, A.E., 1997, Multiple reactivations of accreted terrane boundaries: An example from the Carolina terrane, Brookneal, Virginia, *in* Glover, L., III, and Gates, A.E., eds., Central and Southern Appalachian Sutures: Results of the EDGE Project and Related Studies: Geological Society of America Special Paper 314, p. 49–63, doi:10.1130/0-8137-2314-0.49.
- Gates, A.E., Speer, J.A., and Pratt, T.L., 1988, The Alleghanian southern Appalachian Piedmont: A transpressional model: Tectonics, v. 7, p. 1307–1324, doi:10.1029/TC007i006p01307.
- Ghosh, A., and Holt, W.E., 2012, Plate motions and stresses from global dynamic models: Science, v. 335, p. 838–843, doi:10.1126/science.1214209.
- Ghosh, A., Holt, W.E., and Flesch, L.M., 2009, Contribution of gravitational potential energy differences to the global stress field: Geophysical Journal International, v. 179, p. 787–812, doi:10.1111/j.1365-246X.2009.04326.x.
- Graizer, V., Munson, C.G., and Li, Y., 2013, North Anna nuclear power plant strong-motion records of the Mineral, Virginia, earthquake of

Aftershocks illuminate the 2011 Mineral, Virginia, earthquake causative fault zone

- 23 August 2011: Seismological Research Letters, v. 84, p. 551–557, doi:10.1785/0220120138.
- Harris, L.D., deWitt, W., Jr., and Bayer, K.C., 1982, Interpretive Seismic Profile along Interstate I-64 from the Valley and Ridge to the Coastal Plain in Central Virginia: U.S. Geological Survey Oil and Gas Investigations Chart OC-123, scale 1:25000.
- Harris, L.D., de Witt, W., Jr., and Bayer, K.C., 1986, Interpretive Seismic Profile along Interstate 64 in Central Virginia from the Valley and Ridge to the Coastal Plain: Virginia Department of Mines Minerals and Energy, Division of Mineral Resources Publication 66.
- Heller, M.J., and Carter, A.M., 2015, this volume, Residential property damage in the epicentral area of the Mineral, Virginia, earthquake of August 23, 2011, in Horton, J.W., Jr., Chapman, M.C., and Green, R.A., eds., The 2011 Mineral, Virginia, Earthquake, and Its Significance for Seismic Hazards in Eastern North America: Geological Society of America Special Paper 509, doi:10.1130/2015.2509(10).
- Herrmann, R.B., 2011, Saint Louis University Earthquake Center website: http://www.eas.slu.edu/eqc/eqc_mt/MECH.NA/20110823175105/index.html (March 2014).
- Hibbard, J.P., Van Staal, C.R., and Rankin, D.W., 2007, A comparative analysis of pre-Silurian crustal building blocks of the northern and southern Appalachian orogeny: American Journal of Science, v. 307, p. 23–45, doi:10.2475/01.2007.02.
- Hibbard, J.P., Beard, J.S., Henika, W.S., and Horton, J.W., Jr., 2014, Geology of the Western Piedmont in Virginia, in Bailey, C.M., Sherwood, W.C., Eaton, L.S., and Powars, D.S., eds., The Geology of Virginia: Martinsville, Virginia Museum of Natural History, p. 39–75 (in press).
- Horton, J.W., Jr., and Williams, R.A., 2012, The 2011 Virginia earthquake: What are scientists learning?: Eos (Transactions, American Geophysical Union), v. 93, no. 33, p. 317–318, http://www.agu.org/pubs/pdf/2012EO330001_rga.pdf, doi:10.1029/2012EO330001.
- Horton, J.W., Jr., Drake, A.A., Jr., and Rankin, D.W., 1989, Tectonostratigraphic terranes and their Paleozoic boundaries in the central and southern Appalachians, in Dallmeyer, R.E., ed., Terranes in the Circum-Atlantic Paleozoic Orogens: Geological Society of America Special Paper 230, p. 213–245, doi:10.1130/SPE230-p213.
- Horton, J.W., Jr., Drake, A.A., Jr., Rankin, D.W., and Dallmeyer, R.D., 1991, Preliminary Tectonostratigraphic Terrane Map of the Central and Southern Appalachians: U.S. Geological Survey Miscellaneous Investigations Map I-2163, scale 1:2,000,000.
- Horton, J.W., Jr., Aleinikoff, J.N., Drake, A.A., Jr., and Fanning, C.M., 2010, Ordovician volcanic-arc terrane in the Central Appalachian Piedmont of Maryland and Virginia: SHRIMP U-Pb geochronology, field relations, and tectonic significance, in Tollo, R.P., Bartholomew, M.J., Hibbard, J.P., and Karabinos, P.M., eds., From Rodinia to Pangea: The Lithotectonic Record of the Appalachian Region: Geological Society of America Memoir 206, p. 621–660, doi:10.1130/2010.1206(25).
- Horton, J.W., Jr., Chapman, M.C., Carter, A.M., Carter, M.W., Harrison, R.W., Herrmann, R.B., and Snyder, S.L., 2012a, Faults delineated by aftershocks associated with the 2011 central Virginia earthquake and their tectonic setting: Geological Society of America Abstracts with Programs, v. 44, no. 4, p. 14.
- Horton, J.W., Jr., McNamara, D.E., Shah, A.K., Gilmer, A.K., Carter, A.M., Burton, W.C., Harrison, R.W., Carter, M.W., Herrmann, R.B., and Snyder, S.L., 2012b, Preliminary analysis of magnitude 5.8 Virginia earthquake causative fault and subsidiary faults illuminated by aftershocks: Geological Society of America Abstracts with Programs, v. 44, no. 7, p. 381.
- Horton, J.W., Jr., Owens, B.E., Hackley, P.C., Burton, W.C., Sacks, P.E., and Hibbard, J.P., 2014, Geology of the Eastern Piedmont in Virginia, in Bailey, C.M., Sherwood, W.C., Eaton, L.S., and Powars, D.S., eds., The Geology of Virginia: Martinsville, Virginia Museum of Natural History, p. 76–109 (in press).
- Horton, J.W., Jr., Chapman, M.C., and Green, R.A., 2015, this volume, The 2011 Mineral, Virginia, earthquake and its significance for seismic hazards in eastern North America—Overview and synthesis, in Horton, J.W., Jr., Chapman, M.C., and Green, R.A., eds., The 2011 Mineral, Virginia, Earthquake and its Significance for Seismic Hazards in Eastern North America: Geological Society of America Special Paper 509, doi:10.1130/2015.2509(01).
- Hough, S.E., 2012, Initial assessment of the intensity distribution of the 2011 M_w 5.8 Mineral, Virginia Earthquake: Seismological Research Letters, v. 83, p. 649–657, doi:10.1785/0220110140.
- Hughes, S., and Hibbard, J., 2012a, Relict Paleozoic faults in the epicentral area of the August 23, 2011 Virginia earthquake; geology in the Ferncliff, VA quadrangle: Geological Society of America Abstracts with Programs, v. 44, no. 4, p. 14 (with online handout, 29 slides): https://gsa.confex.com/gsa/2012SE/finalprogram/abstract_202175.htm.
- Hughes, S., and Hibbard, J., 2012b, Relict Paleozoic faults in the epicentral area of the August 23, 2011 Virginia earthquake: Assessing potential sources of reactivation with field observations: Geological Society of America Abstracts with Programs, v. 44, no. 7, p. 380.
- Hughes, K.S., Hibbard, J.P., and Miller, B.V., 2013, Relationship between the Ellisville pluton and Chopawamsic fault: Establishment of significant Late Ordovician faulting in the Appalachian Piedmont of Virginia: American Journal of Science, v. 313, p. 584–612, doi:10.2475/06.2013.03.
- Jordan, T.H., and Sverdrup, K.A., 1981, Teleseismic location techniques and their application to earthquake clusters in the south-central Pacific: Seismological Society of America Bulletin, v. 71, p. 1105–1130.
- Kim, W., and Chapman, M., 2005, The 9 December 2003 central Virginia earthquake sequence: A compound earthquake in the Central Virginia Seismic Zone: Seismological Society of America Bulletin, v. 95, p. 2428–2445, doi:10.1785/0120040207.
- Leonard, M., 2010, Earthquake fault scaling; self-consistent relating of rupture length, width, average displacement, and moment release: Seismological Society of America Bulletin, v. 100, p. 1971–1988, doi:10.1785/0120090189.
- Li, Y., Stirewalt, G.L., and Manoly, K.A., 2015, this volume, Overview of North Anna nuclear power plant's earthquake performance, design basis earthquake, design margin and continued seismic evaluations, in Horton, J.W., Jr., Chapman, M.C., and Green, R.A., eds., The 2011 Mineral, Virginia, Earthquake and its Significance for Seismic Hazards in Eastern North America: Geological Society of America Special Paper 509, doi:10.1130/2015.2509(11).
- Lindholm, R.C., 1978, Triassic-Jurassic faulting in eastern North America—A model based on pre-Triassic structures: Geology, v. 6, p. 365–368, doi:10.1130/0091-7613(1978)6<365:TFIENA>2.0.CO;2.
- Marr, J.D., Jr., 2002, Geologic map of the western portion of the Richmond 30 × 60 minute quadrangle, Virginia: Virginia Division of Mineral Resources Publication 165, scale 1:100,000.
- Mazzotti, S., and Townend, J., 2010, State of stress in central and eastern North American seismic zones: Lithosphere, v. 2, no. 2, p. 76–83, doi:10.1130/L65.1.
- McHone, J.G., 1988, Tectonic and paleostress patterns of Mesozoic intrusions in eastern North America, in Manspeizer, W., ed., Triassic-Jurassic Rifting, Continental Breakup and the Origin of the Atlantic Ocean and Passive Margins, Part B: Developments in Geotectonics 22: New York, Elsevier, p. 607–620.
- McHone, J.G., 2000, Non-plume magmatism and rifting during the opening of the Central Atlantic Ocean: Tectonophysics, v. 316, p. 287–296, doi:10.1016/S0040-1951(99)00260-7.
- McLaren, M.K., Hardebeck, J.L., van der Elst, N., Unruh, J., Bawden, G.W., and Blair, J.L., 2008, Complex faulting associated with the 22 December 2003 M_w 6.5 San Simeon, California, earthquake, aftershocks, and post-seismic surface deformation: Seismological Society of America Bulletin, v. 98, p. 1659–1680, doi:10.1785/0120070088.
- McNamara, D.E., Benz, H.M., Herrmann, R.B., Bergman, E.A., Earle, P., Meltzer, A., Withers, M., and Chapman, M., 2014a, The M_w 5.8 Mineral, Virginia, earthquake of August 2011 and aftershock sequence: Constraints on earthquake source parameters and fault geometry: Seismological Society of America Bulletin, v. 104, p. 40–54, doi:10.1785/0120130058.
- McNamara, D.E., Gee, L., Benz, H.M., and Chapman, M., 2014b, Frequency-dependent seismic attenuation in the eastern United States as observed from the 2011 central Virginia earthquake and aftershock sequence: Seismological Society of America Bulletin, v. 104, p. 55–72, doi:10.1785/0120130045.
- Mixon, R.B., Pavlides, L., Powars, D.S., Froelich, A.J., Weems, R.E., Schindler, J.S., Newell, W.L., Edwards, L.E., and Ward, L.W., 2000, Geologic map of the Fredericksburg 30' × 60' quadrangle, Virginia and Maryland: U.S. Geological Survey Miscellaneous Investigations Series Map I-2607, scale 1:100,000, 34 p.
- Mixon, R.B., Pavlides, L., Horton, J.W., Jr., Powars, D.S., and Schindler, J.S., 2005, Geologic map of the Stafford quadrangle, Stafford County, Virginia: U.S. Geological Survey Scientific Investigations Map 2841, scale 1:24,000, <http://pubs.usgs.gov/sim/2005/2841/>.

- Munsey, J.W., and Bollinger, G.A., 1985, Focal mechanism analyses for Virginia earthquakes: *Seismological Society of America Bulletin*, v. 75, p. 1613–1636.
- Neuschel, S.K., 1970, Correlation of aeromagnetism and aeroradioactivity with lithology in the Spotsylvania area, Virginia: *Geological Society of America Bulletin*, v. 81, p. 3575–3589, doi:10.1130/0016-7606(1970)81[3575:COAAAW]2.0.CO;2.
- Obermeier, S.F., and McNulty, W.E., 1998, Paleoliquefaction evidence for quiescence in central Virginia during late and middle Holocene time: *Eos (Transactions, American Geophysical Union)*, v. 79, no. 17, p. 342.
- Pavlidis, L., 1989, Early Paleozoic composite mélange terrane, central Appalachian Piedmont, Virginia and Maryland; its origin and tectonic history, in Horton, J.W., Jr., and Rast, N., eds., *Mélanges and Olistostromes of the U.S. Appalachians*: *Geological Society of America Special Paper 228*, p. 135–194, doi:10.1130/SPE228-p135.
- Pavlidis, L., Bobyarchick, A.R., and Wier, K.E., 1980, Spotsylvania Lineament of Virginia: U.S. Geological Survey Professional Paper 1175, 73 p.
- Pavlidis, L., Arth, J.G., Sutter, J.F., Stern, T.W., and Cortesini, H., 1994, Early Paleozoic Alkaline and Calc-alkaline Plutonism and Associated Contact Metamorphism, Central Virginia Piedmont: U.S. Geological Survey Professional Paper 1529, 147 p.
- Pazzaglia, F.J., and Brandon, M.T., 1996, Macrogeomorphic evolution of the post-Triassic Appalachian Mountains determined by deconvolution of the offshore basin sedimentary record: *Basin Research*, v. 8, p. 255–278, doi:10.1046/j.1365-2117.1996.00274.x.
- Pazzaglia, F.J., and Gardner, T.W., 1994, Late Cenozoic flexural deformation of the middle U.S. Atlantic passive margin: *Journal of Geophysical Research*, v. 99, no. B6, p. 12143–12157, doi:10.1029/93JB03130.
- Petersen, M.D., Frankel, A.D., Harmsen, S.C., Mueller, C.S., Haller, K.M., Wheeler, R.L., Wesson, R.L., Zeng, Y., Boyd, O.S., Perkins, D.M., Luco, N., Field, E.H., Wills, C.J., and Rukstales, 2008, Documentation for the 2008 Update of the United States National Seismic Hazard Maps: U.S. Geological Survey Open-File Report 2008-1128, 61 p.
- Powars, D.S., Catchings, R.D., and Horton, J.W., Jr., 2012, Stafford fault system: Investigating paleoseismicity in Virginia: *Geological Society of America Abstracts with Programs*, v. 44, no. 7, p. 593.
- Pratt, T.L., 2012, Kinematics of the New Madrid seismic zone, central United States, based on stepover models: *Geology*, v. 40, p. 371–374, doi:10.1130/G32624.1.
- Pratt, T.L., Çoruh, C., Costain, J.K., and Glover, L., III, 1988, A geophysical study of the Earth's crust in central Virginia: Implications for Appalachian crustal structure: *Journal of Geophysical Research*, v. 93, no. B6, p. 6649–6667, doi:10.1029/JB093iB06p06649.
- Pratt, T.L., Horton, J.W., Jr., Spears, D.B., Gilmer, A.K., and McNamara, D.E., 2015, this volume, The 2011 Virginia M5.8 earthquake: Insights from seismic-reflection imaging into influence of older structures on eastern U.S. seismicity, in Horton, J.W., Jr., Chapman, M.C., and Green, R.A., eds., *The 2011 Mineral, Virginia, Earthquake and its Significance for Seismic Hazards in Eastern North America*: *Geological Society of America Special Paper 509*, doi:10.1130/2015.2509(16).
- Robinson, G.R., 1979, Pegmatite cutting mylonite—Evidence supporting pre-Triassic faulting along the western border of the Danville Triassic basin, southern Virginia: *Geological Society of America Abstracts with Programs*, v. 11, p. 210.
- Saint Louis University Earthquake Center, 2013, August 23, 2011 Virginia: <http://www.eas.slu.edu/eqc/eqc20110823.html> (May 2013).
- Schindler, J.S., Harrison, R.W., and Obermeier, S.F., 2012, Review and update of paleoliquefaction evidence for Holocene seismic activity in the Central Virginia seismic zone [abs.]: *Conference Program and Abstracts, 84th Annual Meeting of the Eastern Section of the Seismological Society of America*, Blacksburg, Virginia, Oct. 28–30, 2012, p. 43: http://www.magma.geos.vt.edu/vtso/esssa2012/Program_2012_final.pdf (September 2014).
- Shah, A.J., Horton, J.W., Jr., Harrison, R.W., and Snyder, S.L., 2012a, Magnetic and gravity data constrain geologic features associated with the August 23, 2011 earthquake in Louisa County, Virginia: *Geological Society of America Abstracts with Programs*, v. 44, no. 4, p. 61.
- Shah, A.K., Horton, J.W., Jr., and Gilmer, A.K., 2012b, Airborne magnetic, gravity and radiometric data illuminate subsurface geology associated with the M5.8 August 23, 2011 Louisa County, VA earthquake: *Geological Society of America Abstracts with Programs*, v. 44, no. 7, p. 381.
- Shah, A.K., Horton, J.W., and Gilmer, A.K., 2012c, Airborne geophysical surveys used to delineate geological features associated with the M5.8 August 23, 2011 earthquake in Louisa County, Virginia: *American Geophysical Union, 2012 Fall Meeting*, San Francisco, California, 3–7 December, abs. GP42A–03.
- Shah, A.K., Horton, J.W., Jr., Burton, W.C., Spears, D.B., and Gilmer, A.K., 2015, this volume, Subsurface geologic features of the 2011 central Virginia earthquakes revealed by airborne geophysics, in Horton, J.W., Jr., Chapman, M.C., and Green, R.A., eds., *The 2011 Mineral, Virginia, Earthquake and its Significance for Seismic Hazards in Eastern North America*: *Geological Society of America Special Paper 509*, doi:10.1130/2015.2509(17).
- Shearer, P.M., Hardebeck, J.L., Astiz, L., and Richards-Dinger, K.B., 2003, Analysis of similar event clusters in aftershocks of the 1994 Northridge, California, earthquake: *Journal of Geophysical Research*, v. 108, no. B1, 2035, doi:10.1029/2001JB000685.
- Sherrod, B.L., Brocher, T.M., Weaver, C.S., Bucknam, R.C., Blakely, R.J., Kelsey, H.M., Nelson, A.R., and Haugerud, R., 2004, Holocene fault scarps near Tacoma, Washington, USA: *Geology*, v. 32, p. 9–12, doi:10.1130/G19914.
- Snyder, S.L., 2005, Virginia aeromagnetic and gravity maps and data: A web site for distribution of data: U.S. Geological Survey Open-File Report 2005-1052, <http://pubs.usgs.gov/of/2005/1052/> (May 2013).
- Spears, D.B., 2011, Geology of the Lakeside Village quadrangle, Virginia: Virginia Division of Geology and Mineral Resources Publication 177, 19 p.
- Spears, D.B., and Bailey, C.M., 2002, Geology of the Central Virginia Piedmont Between the Arvonian Syncline and the Spotsylvania High-Strain Zone: *Virginia Geological Field Conference Guidebook 32*, 36 p.
- Spears, D.B., and Gilmer, A.K., 2012, Preliminary findings from recent geologic mapping in the Central Virginia seismic zone: *Geological Society of America Abstracts with Programs*, v. 44, no. 7, p. 593.
- Spears, D.B., Owens, B.E., and Bailey, C.M., 2004, The Goochland-Chopawamsic terrane boundary, central Virginia Piedmont, in Southworth, C.S., and Burton, W., eds., *Geology of the National Capital Region—Field Trip Guidebook*: U.S. Geological Survey Circular 1264, p. 223–245.
- Spears, D.B., Evans, N.H., and Gilmer, A.K., 2013, Geologic Map of the Pendleton Quadrangle, Virginia: Virginia Department of Mines, Minerals and Energy, Division of Geology and Mineral Resources, 2013 STATEMAP deliverable, scale 1:24,000 (available on request from Virginia Division of Geology and Mineral Resources).
- Stein, S., Cloetingh, S., Sleep, N., and Wortel, R., 1989, Passive margin earthquakes, stresses, and rheology, in Gregerson, S., and Basham, P.W., eds., *Earthquakes at North Atlantic Passive Margins: Neotectonics and Post-glacial Rebound*: Dordrecht, Netherlands, Kluwer Academic Publishers, p. 231–260.
- Stewart, I.S., Sauber, J., and Rose, J., 2000, Glacio-seismotectonics: Ice sheets, crustal deformation and seismicity: *Quaternary Science Reviews*, v. 19, p. 1367–1389, doi:10.1016/S0277-3791(00)00094-9.
- Swanson, M.T., 1986, Preexisting fault control for Mesozoic basin formation in eastern North America: *Geology*, v. 14, p. 419–422, doi:10.1130/0091-7613(1986)14<419:PFCFMB>2.0.CO;2.
- Sykes, L.R., 1978, Intraplate seismicity, reactivation of preexisting zones of weakness, alkaline magmatism, and other tectonism postdating continental fragmentation: *Reviews of Geophysics and Space Physics*, v. 16, p. 621–688, doi:10.1029/RG016i004p0621.
- Tarr, A.C., and Wheeler, R.L., 2006, Earthquakes in Virginia and vicinity 1774–2004: U.S. Geological Survey Open-File Report 2006-1017, Version 1.0, 1 sheet, <http://pubs.usgs.gov/of/2006/1017/> (May 2013).
- Thomas, W.A., 2006, Tectonic inheritance at a continental margin: *GSA Today*, v. 16, no. 2, p. 4–11, doi:10.1130/1052-5173(2006)016[4:TIAACM]2.0.CO;2.
- U.S. Geological Survey, 2012, Aug. 23, 2011 M5.8 Virginia Earthquake Aftershocks: U.S. Geological Survey Earthquake Hazards Program, http://earthquake.usgs.gov/earthquakes/states/events/2011_08_23/ (September 2014).
- U.S. Geological Survey, 2013, National Earthquake Information Center—NEIC: U.S. Geological Survey Earthquake Hazards Program, <http://earthquake.usgs.gov/regional/neic/> (July 2013).
- U.S. Geological Survey and National Geophysical Data Center, 2002, Digital aeromagnetic datasets for the conterminous United States and Hawaii—A companion to the North American Magnetic Anomaly Map: U.S. Geological Survey Open-File Report 02-361, version 1.0, <http://pubs.usgs.gov/of/2002/ofr-02-361/> (May 2013).
- Virginia Division of Mineral Resources, 1993, Geologic Map of Virginia: Virginia Division of Mineral Resources, scale: 1:500,000.

Aftershocks illuminate the 2011 Mineral, Virginia, earthquake causative fault zone

- Wald, D.J., Quitoriano, V., Worden, C.B., Hopper, M., and Dewey, J.W., 2011, USGS "Did You Feel It?" Internet-based macroseismic intensity maps: *Annals of Geophysics*, v. 54, p. 6, doi:10.4401/ag-5354.
- Wells, D.L., and Coppersmith, K.J., 1994, New empirical relationships among magnitude, rupture length, rupture width, rupture area, and surface displacement: *Seismological Society of America Bulletin*, v. 84, p. 974–1002.
- Wilkes, G.P., 1982, Geology and mineral resources of the Farmville Triassic basin, Virginia: *Virginia Minerals*, v. 28, p. 25–32.
- Withjack, M.O., Schlische, R.W., and Olsen, P.E., 2012, Development of the passive margin of Eastern North America: Mesozoic rifting, igneous activity, and breakup, *in* Roberts, D.G., and Bally, A.W., eds., *Phanerozoic Rift Systems and Sedimentary Basins*: Amsterdam, Netherlands, Elsevier, p. 301–335, doi:10.1016/B978-0-444-56356-9.00012-2.
- Wolin, E., Stein, S., Pazzaglia, F., Meltzer, A., Kafka, A., and Berti, C., 2012, Mineral, Virginia, earthquake illustrates seismicity of a passive-aggressive margin: *Geophysical Research Letters*, v. 39, L02305, doi:10.1029/2011GL050310.
- Zhang, P.-Z., Wen, X., Shen, Z.-K., and Chen, J., 2010, Oblique, high-angle listric-reverse faulting and associated development of strain: The Wenchuan earthquake of May 12, 2008, Sichuan China: *Annual Review of Earth and Planetary Sciences*, v. 38, p. 353–382, doi:10.1146/annurev-earth-040809-152602.
- Zietz, I., Calver, J.L., Johnson, S.S., and Kirby, J.R., 1977, Aeromagnetic map of Virginia: U.S. Geological Survey Geophysical Investigation Map GP-915, scale 1:500,000.
- Zoback, M.L., 1992, Stress field constraints on intraplate seismicity in eastern North America: *Journal of Geophysical Research*, v. 97, no. B8, p. 11,761–11,782, doi:10.1029/92JB00221.

MANUSCRIPT ACCEPTED BY THE SOCIETY 6 JUNE 2014

Geological Society of America Special Papers Online First

Aftershocks illuminate the 2011 Mineral, Virginia, earthquake causative fault zone and nearby active faults

J. Wright Horton, Jr., Anjana K. Shah, Daniel E. McNamara, et al.

Geological Society of America Special Papers, published online November 26, 2014;
doi:10.1130/2015.2509(14)

E-mail alerting services click www.gsapubs.org/cgi/alerts to receive free e-mail alerts when new articles cite this article

Subscribe click www.gsapubs.org/subscriptions to subscribe to Geological Society of America Special Papers

Permission request click www.geosociety.org/pubs/copyrt.htm#gsa to contact GSA.

Copyright not claimed on content prepared wholly by U.S. government employees within scope of their employment. Individual scientists are hereby granted permission, without fees or further requests to GSA, to use a single figure, a single table, and/or a brief paragraph of text in subsequent works and to make unlimited copies of items in GSA's journals for noncommercial use in classrooms to further education and science. This file may not be posted to any Web site, but authors may post the abstracts only of their articles on their own or their organization's Web site providing the posting includes a reference to the article's full citation. GSA provides this and other forums for the presentation of diverse opinions and positions by scientists worldwide, regardless of their race, citizenship, gender, religion, or political viewpoint. Opinions presented in this publication do not reflect official positions of the Society.

Notes